Aerial transmission of SARS-CoV-2 virus (and pathogens in general) through environmental e-cigarette aerosol

Roberto A Sussman[1], Eliana Golberstein[b], Riccardo Polosa[c]

[a]*Instituto de Ciencias Nucleares, Universidad Nacional Autónoma de México, Ciudad de México, 04510, México*
[b]*Myriad Pharmaceuticals Limited, Unit 3, 36 Greenpark Rd, Penrose, 1061, Auckland, New Zealand*
[c]*Center of Excellence for the acceleration of HArm Reduction (CoEHAR) University of Catania, Italy*

Abstract

We examine the plausibility, scope and risks of aerial transmission of pathogens (including the SARS-CoV-2 virus) through respiratory droplets carried by exhaled e–cigarette aerosol (ECA). Observational and laboratory data suggests considering cigarette smoking and mouth breathing through a mouthpiece as convenient proxies to infer the respiratory mechanics and droplets sizes and their rate of emission that should result from vaping. To quantify direct exposure distance we model exhaled ECA flow as an intermittent turbulent jet evolving into an unstable puff, estimating for low intensity vaping (practiced by 80-90 % of vapers) the emission of 6-200 (mean 79.82, standard deviation 74.66) respiratory submicron droplets per puff a horizontal distance spread of 1-2 meters, with intense vaping possibly emitting up to 1000 droplets per puff in the submicron range a distance spread over 2 meters. Since exhaled ECA acts effectively as a visual tracer of its expiratory flow (because of its dynamical and optical properties) bystanders become instinctively aware that possible direct contagion might occur only in the direction and scope of the jet. In a home or restaurant scenarios without face mask wearing bystanders exposed to ECA expirations by an infectious vaper face a 1 % increase of risk of contagion with respect to a "control case" scenario defined by exclusively rest breathing without vaping. This relative added risk becomes $5 - 17$ % for high intensity vaping, $44 - 176$ % and over 260 % for speaking for various periods or coughing (all without vaping). Face masks of common usage effectively protect wearers from respiratory droplets possibly emitted by mask-less vapers as long as they avoid direct exposure to the visible exhaled vaping jet. We estimate that disinfectant properties of glycols in ECA are unlikely to act efficiently on pathogens carried by vaping expirations under realistic conditions.

Keywords: SARS-CoV-2 COVID-19, electronic cigarettes, droplet dynamics, risk modeling

1. Introduction

The current COVID-19 pandemic has brought justified concern and attention to aerial disease contagion through bioaerosols. This contagion is conventionally classified in two modalities determined by the diameter of the aqueous droplets carrying the pathogens, with direct *close range* exposure associated with large droplets (denoted as "droplets") that rapidly settle at short

*Corresponding author
Email address: sussman@nucleares.unam.mx (Roberto A Sussman)

distances and *airborne* indirect exposure to small droplets (denoted as "aerosols") that evaporate before settling, thus remaining buoyant for long periods and spreading large distances, with 5 μm being the conventional cut–off diameter between these two modalities [1] .

There is currently a broad consensus, endorsed by the WHO Organization et al. (2020) and the CDC Brief (2020), that available data supports the occurrence of direct contagion of the SARS-CoV-2 virus by close range exposure to relatively large droplets emitted by infectious invididuals. While there is also a broad consensus on the factual occurrence of contagion through indirect exposure to smaller submicron droplets (for example Liu et al. (2020); Li et al. (2020); Lu et al. (2020); Cai et al. (2020); Shen et al. (2020)), its scope and relevance still remains controversial Klompas et al. (2020); Morawska and Milton (2020); Morawska and Cao (2020); NAS (2020); Jayaweera et al. (2020); Shiu et al. (2019).

The evolution of bioaerosols spreading disease contagion through respiratory droplets has been widely studied, as can be appreciated in reviews on generic pathogens Gralton et al. (2011); Zhang et al. (2015), the influenza Weber and Stilianakis (2008) and SARS Yu et al. (2004) viruses and in spread risk modeling Sze To et al. (2008) (see the chapter on bioaerosols in Ruzer and Harley (2012) and cited references therein for a full recount of the literature up to 2013). As expected, the current COVID-19 pandemic has motivated the study of direct and indirect aerial transmission of the SARS–CoV–2 virus through various expiratory activities, such as breathing, whispering, speaking, singing, coughing and sneezing.

The purpose of the present paper is to fill an important gap in the above mentioned body of literature on pathogen (including SARS-CoV-2) transmission by the spread of respiratory droplets, namely: to examine the plausibility, scope and risks of this transmission through a different expiratory route: exhaled e–cigarette aerosol (ECA). As far as we are aware, not only there is no previous proper research on this topic, but there is currently no factual evidence that pathogens have been spread through this route. However, we hypothesize that this transmission is entirely plausible simply because vaping (usage of e-cigarettes) is an expiratory activity (as well as smoking [2]).

The relevance of the present paper can be appreciated by bearing in mind that the current COVID-19 pandemic affects millions of vapers and non-users surrounding them (as well as smokers), either confined in their homes under lockdown or subjected to preventive measures when conditions allow partial reopening of the economy. Objective research on COVID-19 transmission through exhaled ECA can serve to guide evidence based public policies to address public health concerns and risk management and minimization. When data and direct evidence is unavailable (as in this case), public policies must be based on available theoretical knowledge and solid inference from indirect evidence. Given the relevance of assessing contagion risks in the context of the COVID-19 pandemic, we have written a short related article Sussman et al. (2020) with the purpose of focusing on its public health and public policy implications.

It is necessary to issue the following important disclaimer: the present article is concerned

[1] The 5 μm cut–off cutoff is a purely conventional value not based on any specific property of aerosol physics. It simplifies droplet dynamical properties that vary along a continuous spectrum of diameters into two mutually exclusive modalities. We will avoid altogether the "droplets" vs "aerosols" terminology, with the term "droplets" referring henceforth to generic respiratory droplets of continuously varying diameters.

[2] This paper will not address potential COVID-19 contagion through respiratory droplets carried by environmental tobacco smoke, though smoking can serve as a useful proxy for understanding the respiratory and dynamical parameters of low intensity ('mouth to lung') puffing style practiced by 80-90 % of vapers. However, most of the results we obtain are applicable to "mainstream" smoke exhalations emitted by smokers, not to sidestream emissions from the burning/smouldering tip of cigarettes, cigars and pipes that make the bulk of environmental tobacco smoke.

only with the plausibility, scope and risks of SARS-CoV-2 transmission through exhaled ECA, not with vaping as a possible risk factor for becoming infected by the virus or for any evolution or stage of adverse health outcomes associated with COVID19. Also, we will not be concerned with possible health hazzards by users' exposure to inhaled ECA or bystanders to exhaled ECA derived from the usage of e-cigarettes as substitute of tobacco smoking. Readers are advised to consult the available literature on these subjects (see extensive reviews Farsalinos and Polosa (2014); RCP (2016); McNeill et al. (2018); Daynard (2018); Polosa et al. (2019)).

In what follows we provide a section by section summary of the paper that illustrates its methodological structure:

Background: Section 2. Vaping styles and demographics (subsection 2.1); Physical properties of inhaled and exhaled ECA (subsection 2.2); Exhaled ECA as a marker of expiratory fluid flow (subsection 2.3).

Methods I: Section 3. The lack of experimental evidence on respiratory droplets potentially carried by ECA requires inferring their characteristics through appropriate respiratory proxies on which such evidence exists. To accomplish this task we undertake the following steps: Discuss the usage of cigarette smoking as a proxy for respiratory mechanics of vaping (subsection 3.1). Vaping involves suction through a mouthpieces, whose effects on respiratory mechanics need to be examined (subsection 3.2). We provide arguments to show that mouth breathing is an appropriate proxy to infer ECA droplet emission that should result from vaping (subsection 3.3).

Methods II: Assessing exposure. We estimate the horizontal spread of droplets in exhaled ECA by modeling its flow as a turbulent jet with finite injection evolving into an unstable puff (section 4). To infer risks for volume (direct and indirect) exposure to the SARS-CoV-2 virus we incorporate vaping exhalations into a simplified version of the exponential dose-response reaction model developed by Buonanno, Morawska and Stabile Buonanno et al. (2020a) (section 5). We examine the experimental evidence on the disinfectant properties of ECA that could affect respiratory droplets (section 6).

Results: Section 7:

- Subsection 7.1: *Respiratory droplets potentially carried by ECA*. Low intensity vaping should produce exhalations of mean tidal volume of $700-900\,\mathrm{cm}^3$, emitting 6–200 droplets per puff (mean 79.92, SD 74.66) overwhelmingly in the submicron range. High intensity vaping involves exhaled volumes between $1000-3000\,\mathrm{cm}^3$ and possible emission between several hundreds up to over 1000 droplets also in the submicron range.

- Subsection 7.2: *Visualization of expiratory flows through exhaled ECA*. This important feature follows from its optical properties: light extinction and scattering by aerosol droplets. We discuss how these properties (together with the fluid dynamical properties discussed in section 2.3) explain why expirations from vaping can be seen while those from other respiratory activities cannot.

- Subsection 7.3: *Distance for direct exposure.* The jet/puff hydrodynamical model presented in section 4 yields a horizontal distance spread between $0.5 - 2,0$ meters (low intensity vaping) and over 2 meters (high intensity) in the direction of the exhaled jet.

- Subsection 7.4: *Exposure risks in indoor spaces without face mask wearing.* We find that the intermittent nature of vaping drastically reduces the added relative contagion risk with

respect to the control case of exclusive rest breathing. For a home and restaurant indoor spaces exposure to low intensity vaping just adds about 1 % extra risk with respect to the control case scenario. For high intensity vaping this added relative risk is of the order of $5 - 17$ %, while it rises to $44 - 90$ % and over 260 % if for exposure to vocalizing and coughing (without vaping). Mechanical ventilation significantly reduces absolute exposure risks but keeps the same relative risks.

- Subsection 7.5: *Risks with universal face mask wearing.* Vaping requires mask removal for (at least) short intermittent periods. However, bystanders wearing face masks would be effectively protected from these mask free emissions by locating themselves away from the zone of direct exposure delineated by the visual vaping jet.

- Subsection 7.6: *ECA as disinfectant.* An examination of the experimental outcomes presented in section 6 suggests that propylene glycol contained in ECA is not likely to affect respiratory droplets under the conditions of normal e–cigarette usage. Nevertheless, appropriate experiments should be set up to probe this possibility even outside the context of vaping.

We conclude the paper by presenting in section 8 its limitations, together with a final thorough discussion.

2. Background

2.1. Vaping styles and demographics

2.1.1. Puffing topography

Vaping is characterized by a wide range of distinct and individualized usage patterns loosely described by the parameters of *puffing topography*: puff and inter puff duration, puff volume and flow Dautzenberg and Bricard (2015); Farsalinos et al. (2018); Spindle et al. (2017); Soulet et al. (2019). This is a factor that complicates the study and evaluation of e–cigarette aerosol (ECA) emissions, more so given the need to upgrade standardization of vaping protocols, specially for the appropriate configuration of vaping machines used for research and regulation.

To simplify the description of vaping style, we consider two vaping topographies: low intensity "Mouth–To–Lung" (MTL), high intensity "Direct–to–Lung" (DTL), described as follows

- MTL. It consists of three stages: (1) "puffing", ECA is sucked orally while breathing through the nose, (2) the puffed ECA is withdrawn from the mouth held in the oropharyngeal cavity without significant exhalation and (3) inhalation into the lungs of the ECA bolus by tidal volume of air from mouth and nose inspiration. It is a low intensity regime involving low powered devices (mostly starting kits, closed systems and recent "pods") roughly similar to the topography of cigarette smoking.

- DTL. As (1) in MTL but bypassing (2): the ECA bolus diluted in tidal volume is inhaled directly into the lung without mouth retention. It is mostly a high intensity regime associated with advanced tank systems.

The topography parameters characterizing these styles are listed in Table 1. It is important to remark that these parameters change when vaping *ad libitum* in natural environments instead of

Parameters of vaping topographies.					
Mouth to Lung (MTL)					
Intensity	m_b	V_b	Φ_b	t_p	V_T
Low	2–10 mg	20–100	20–40	2-5	300–1500
Direct to Lung (DTL)					
Intensity	m_b	V_b	Φ_b	t_p	V_T
High	10–40 mg	300–500	100–300	3–6	1000–3000

Table 1: **Parameters of vaping topography for vaping styles**. Puff topography parameters: m_b, V_b, Φ_b are respectively mass (mg) (aerosol yield), volume (mL), flow (mL/sec) per puff of ECA bolus (aerosol yield). Notice that tidal volume V_T listed in the table is not the tidal volume for quiet rest breathing ($400-600$ mL), since vaping involves suction of ECA through a mouthpiece (see Sections 3.1 and 3.2). Puff time (secs) is t_p. Values taken from from rough representative averages from data in figures 1 and 3 of Spindle et al. (2017) and also from Soulet et al. (2019).

doing so in a laboratory setting. This was reported in Spindle et al. (2017): for example, average puff duration was about 20% longer ad libitum, 5 seconds vs 4 seconds in a laboratory setting.

A third puffing topography not included in Table 1 is "Mouth Puffing": it shares step (1) of MTL but without step (3), with the ECA bolus diluted in tidal volume air being exhaled without lung inhalation. It is a low intensity regime but involving higher exhaled aerosol density, since less than 5% of aerosol mass is deposited in the mouth Asgharian et al. (2018). Very few vapers and cigarette smokers use this style, but most smokers of prime cigars and tobacco pipes do.

2.1.2. Demographics and markets

It is crucial to examine how representative among vapers are the different puff topographies and levels of intensity, something that has varied with time depending on the popularity and availability of different devices. Currently, low powered devices (mostly closed) are the most representative in the largest and most established markets. As shown in figure 1 (Credit to ECig Intelligence Eci (2020)) consumer surveys reveal that the overwhelming majority of vapers (80% in the USA) and 90% in the UK) utilize low powered devices (mostly kits for beginners and closed systems), with advanced open tank systems taking the rest.

2.2. Inhaled and exhaled E-cigarette aerosol (ECA)

The ECA is generated by various physicochemical processes: self–nucleated condensation in a super saturated medium initiates immediately once the e-liquid vapor leaves the coil, the nucleated centers generate small nm scale droplets that grow through coagulation and diffusion Floyd et al. (2018). The particulate phase is made of liquid droplets whose chemical composition closely matches that of the e-liquid: propylene glycol (PG), vegetable glycerin or glycerol (VG), nicotine, water Grégory et al. (2020), together with a trace level contribution of nanometer sized metal particles Mikheev et al. (2016). The gas phase is chemically similar. The aerosol contains nicotine and residues produced from the pyrolysis of the glycols and the flavorings (mainly carbonyls), which can be in either the gas or particulate phase depending on their vapor pressure and volatility Pankow (2017), with most of the PG evaporating into the gas phase and VG tending to be remain in the droplets Grégory et al. (2020).

Count mean diameter (CMD) distributions of mainstream ECA droplets vary depending on the device, puffing style of users, flavors and nicotine content Floyd et al. (2018); Lechasseur

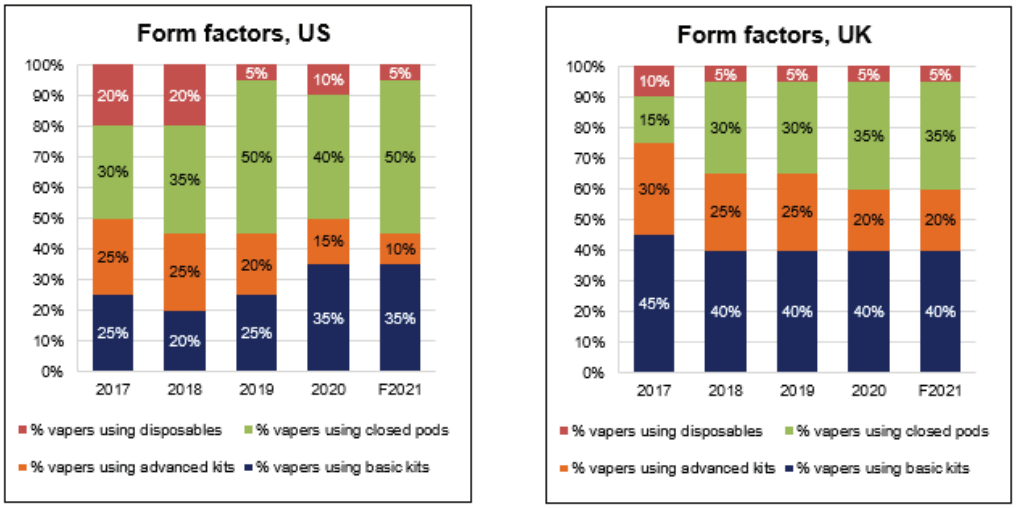

(a) (b)

Figure 1: Usage of different classes of e-cigarette devices in the US and UK markets. Notice that only 15 % and 20 % of consumers in the USA and the UK use advanced kits that allow for the DTL vaping style (Credit to ECig Intelligence Eci (2020)).

et al. (2019). Droplet number count is heavily dominated by submicron droplets with CMD distributions having either single modes below 100 nm or bimodal forms (one mode well below 100 nm and one in the range 100-300 nm) Floyd et al. (2018); Lechasseur et al. (2019); Scungio et al. (2018); Sosnowski and Odziomek (2018); Zhao et al. (2016); Fuoco et al. (2014). However, particle size grows with increasing coil power Lechasseur et al. (2019) and even in low powered devices the mass distribution is dominated by droplets larger than 600 nm Floyd et al. (2018). In fact, Floyd et al. (2018) found a third mode around 1 μm that becomes more prominent at increasing power of the tested device while the nm sized modes decrease, likely because higher power involves larger vaporized mass that favors coagulation and scavenging of nm sized droplets by larger droplets.

The inhaled aerosol mass yield depends on the topography parameters given in Table 1. At inhalation of mainstream ECA instrument measured droplet density numbers are in the range $n = 1 - 5 \times 10^9/\text{cm}^3$ Lechasseur et al. (2019); Scungio et al. (2018); Sosnowski and Odziomek (2018); Zhao et al. (2016); Fuoco et al. (2014). Total average droplet numbers of $N_p = 7.6 \times 10^{10}$ were reported in Manigrasso et al. (2015) for a tank system using e–liquids with high nicotine content in a 2 second machine puff regime [3] with $V_b = 50$ mL puff volume (N_p decreases 25 % with nicotine-free e-liquids). Using the same experimental design Fuoco et al. (2014) reported an increase of up to 30% for 4 second machine puff regime. The estimation $N_p \sim 10^{10} - 10^{11}$ is reasonable given a particle number concentration of $\sim 10^9/\text{cm}^3$ and $V_b = 20 - 100$ mL of low

[3] These machine puff time lapses are different from those reported in Table 1. The former correspond only to inhalation times as instruments aim at simulation of a mouth inhalation, the latter are time lapses in human vapers and thus include inhalation and exhalation.

intensity vaping, with $N_p \sim 10^{12}$ for high intensity vaping with $V_b = 500$ mL.

Data on the gas/particle phase partition of the aerosol mass yield m_b is roughly: 50% Total Particulate Matter (TPM), 40% PG/VG gas phase, 7% water vapor, $< 3\%$ nicotine McAdam et al. (2019), roughly a similar gas/particulate phase partition to that of tobacco smoke Martonen (1992). As shown in Grégory et al. (2020) and Pankow (2017) the presence of compounds in gas or PM form depends on their vapor pressure, with PG tending to be gaseous, VG in PM, for nicotine it depends on its PH, while some aldehydes (like formaldehyde) are most likely in the gas phase.

Values of particle numbers and densities for the exhaled ECA can be estimated by considering its retention by the respiratory system. Retention of $\sim 90\%$ of total inhaled aerosol mass was reported in St. Helen et al. (2016) for a wide variety of devices and e–liquids, with the following average compound specific retention percentages: 86% VG, 92% PG, 94% nicotine, while Samburova et al. (2018) reported 97% total aldehyde retention. This high retention percentages are consistent with the mass distribution of inhaled ECA dominated by larger micron sized droplets which tend to be efficiently deposited in the upper respiratory tracts Floyd et al. (2018). Assuming equal retention rate for the particulate and gas phases, we take as total mass of exhaled aerosol and total numbers of exhaled ECA droplet to be 10 % of the values of m_b listed in Table 1 and 10 % of the values of $N_p = 6.7 \times 10^{10}$ reported in Manigrasso et al. (2015) for a 2 second machine inhalation puff and 50 mL puff volume. Droplet number density of ECA as it is exhaled can be estimated from these values of N_p bearing in mind that the exhaled ECA is now diluted in tidal volumes V_T listed in Table 1 for the various vaping topographies. This yields number densities in the approximate range $n_p = 10^6 - 10^7\,\mathrm{cm}^{-3}$ (lower to higher vaping intensities).

Exhaled ECA dilutes and disperses very fast. Its chemical composition is similar to that of inhaled ECA, both in the gas phase and the droplets Floyd et al. (2018), with PG and water in the latter evaporating rapidly. Since hyperfine nm sized droplets deposit efficiently by diffusion in the alveolar region and larger micron sized droplets (which tend to grow from hygroscopic coagulation Asgharian et al. (2018); Floyd et al. (2018)) deposit by impaction in the upper respiratory tracts Asgharian et al. (2018); Manigrasso et al. (2015); Lechasseur et al. (2019); Sosnowski and Odziomek (2018), the CMD distribution of ECA as it is exhaled should be dominated by modes in intermediate ranges $0.1 - 0.5\,\mu$m. Since there are no ECA measurements at the exhalation point (the vaper's mouth), we can estimate the representative droplet diameter by a rough order of magnitude calculation: assuming an aerosol mass yield of 5 mg of inhaled ECA for a low powered device, a 90% retention of aerosol mass with 50 % made of PM, the total droplet mass of exhaled ECA should be around $M_p = 0.25$ mg. Since 90 % of droplets are retained, the total number of exhaled droplets should be $N_p = 7.6 \times 10^9$ droplets Manigrasso et al. (2015), leading to a median droplet mass of $m_p = M_p/N_p = 3.9 \times 10^{-14}$ gm $= (\pi/6)\rho_p\, d_p^3$, where ρ_p is the droplets density that we can assume to be close to VG density: $\rho_p = 1.3\,\mathrm{gm/cm}^3$, leading to $d_p = 0.38\,\mu$m. Similar order of magnitud values are obtained for the parameters of high intensity vaping.

The fact that CMD chamber measurements are in the range $d_p = 0.1{-}0.2\,\mu$m can be explained by the fact that detectors are located 1-2 meters from the exhalation source, thus measured ECA droplets have already undergone significant degree of dilution and evaporation (as shown in Grégory et al. (2020) droplets' mass can decrease by one third in just 1 second by evaporation of its PG content). This is consistent with droplet number densities dropping at least two orders of magnitud from $\sim 10^6 - 10^7\,\mathrm{cm}^{-3}$ as they are exhaled to $n \sim 10^4 - 10^5\,\mathrm{cm}^{-3}$ at one meter distance from the emission and further dropping to near background levels $n \sim 10^3\,\mathrm{cm}^{-3}$ at two meters Zhao et al. (2017); Martuzevicius et al. (2019); Palmisani et al. (2019).

2.3. **Exhaled ECA as a visual tracer of respiratory fluid flow**

The overwhelmingly submicron droplets that form the particulate phase of ECA have negligible influence on its fluid dynamics, acting essentially as visible tracers or (to a good approximation) as molecular contaminants carried by the fluid. This follows from its basic fluid dynamical characteristic: it is a "single–phase fluid flow" (SFF) system Yeoh and Tu (2019); Elghobashi (1994). As a consequence, ECA droplets visually mark the actual expiratory flow associated with vaping exhalations (we discuss the optical properties that allow for its visualization in section 7.2).

Exhaled ECA is just one among numerous gas markers and aerosols in a SFF regime that serve (and are widely used) to visualize expired air Ai et al. (2020); Nazaroff (2004). This also applies to mainstream exhaled tobacco smoke, whose particulate matter is also made of submicron liquid and solid droplets. In fact, there are studies that have directly used cigarette smoke as a tracer to visualize respiratory airflows Gupta et al. (2009, 2010); Ivanov (2019). Respiratory droplets potentially carried by exhaled ECA would not change its possible role as a tracer of expiratory flows, since as we show further ahead (section 3.3) these droplets are also overwhelmingly in the submicron range and their numbers are several orders of magintude fewer than ECA droplets.

Submicron ECA droplets (whose density should be close to VG density $\rho_p \sim 1.3$ gm/cm^3) are evolving along a carrier fluid made of the gas phase of ECA strongly diluted in exhaled air (in practice, we can think of the carrier fluid simply as exhaled air at mouth temperature $\sim 30 - 35^\circ$ C). In what follows we examine two criteria that determine the SFF character of exhaled ECA: the particles' relaxation time and volume fraction.

Submicron particles in a carrier fluid essentially follow the fluid flow because of their little inertia. They are well within the Stokes regime with Reynolds numbers $Re_p \ll 1$ and negligibly small relaxation times $t_{\rm rel}$, the response time of an aerosol particle to adjust to external forces. For $d_p = 0.3\,\mu$m we get Hinds (1999)

$$t_{\rm rel} = \frac{\rho_p\, d_p^2\, C_c}{18\,\mu} \approx 5.3 \times 10^{-6}\ \text{sec}, \tag{1}$$

where $\mu = 1.895 \times 10^{-5}$gm/(sec cm) the dynamic viscosity of air at 35 C and $C_c = 1 + (\lambda/d_p)[2.34 + 1.05\exp(-0.39 d_p/\lambda)] \approx 1.4$ is the Cunningham slip factor with $\lambda = 0.066\,\mu$m the mean molecular free path of air.

The relaxation time (1) provides the time scale for a particle released into a fluid with velocity U along a horizontal stream to settle into the fluid velocity (neglecting gravity). In this case (see Chapter 3 of Hinds (1999)) the velocity of the particle $v_p(t) = U\,(1 - e^{-t/t_{\rm rel}})$ becomes practically identical to U in about 10^{-5} seconds (instantaneously in practical terms), thus justifying the notion of particles simply following the fluid flow with (practically) no influence on its dynamics.

This behavior occurs also for the larger ECA droplets of $d_p \sim 1\,\mu$m whose relaxation times are $t_{\rm rel} \sim 10^{-4}$ (since $t_{\rm rel} \propto d_p^2$). Evidently, these relaxation times are much smaller than macroscopic characteristic times of the carrier fluid (for example a 2 second inhalation time or even the tenths of a second the ECA stays in the mouth cavity Asgharian et al. (2018)). The Stokes number is defined as $St = t_{\rm rel}/t_f$, where t_f is a characteristic fluid time, hence for the exhaled ECA we have $St \ll 1$, which is another criterion to define SFF systems.

Another criterion for an aerosol to be described as SFF systems is the ratio ϕ of total volume

of the particles to the fluid volume satisfying Yeoh and Tu (2019); Elghobashi (1994)

$$\phi = \frac{N_p V_p}{V_f} < 10^{-6}, \tag{2}$$

where N_p is the total number of particles, $V_p = (\pi/6)d_p^3$ is the particles' volume (assuming they are spherical) and V_f is the fluid volume. Substituting the qualitative values we obtained for the exhaled ECA: $N_p = 7.6 \times 10^9$, $d_p = 0.3\,\mu$m and an exhaled air volume of $V_f = V_T = 300 - 1500$ mL for a low intensity regime yields $\phi = 1{-}3 \times 10^{-7}$, which fulfills (2). This condition holds even if we assume that a large part of the mass distribution is contained in micron sized ($d_p \sim 1\,\mu$m) droplets making (say) 1-10 % of the total number. The value of ϕ is bound to decrease as the exhaled ECA dilutes and the volatile droplet compounds (PG and water) evaporate. As shown in Grégory et al. (2020) this process decreases the droplets mass (and thus volume) to one third while the fluid volume increases and thus ϕ necessarily decreases.

Evidently, larger droplets (diameters larger than a few μm) are present in particle diameter distributions (of both ECA and respiratory droplets) and such particles should contain a significant portion of the aerosol mass Floyd et al. (2018), but they are too few in numbers and deviate from the flow following ballistic trajectories, thus do not affect the dynamics of the carrier fluid to consider ECA as a biphasic fluid flow system.

3. Methods I: Inferences on respiratory droplets spread by ECA

3.1. Vaping as a respiratory process

Tobacco smoke is a valid physical reference for ECA, as it is also an aerosol in a SFF regime characterized by a particulate phase made of predominantly submicron particles with similar particle numbers and diameter distributions Floyd et al. (2018); Sosnowski and Odziomek (2018); Sosnowski and Kramek-Romanowska (2016) (though the particulate and the gas phases of each aerosol have very different chemical properties). This fact, together with the fact that most vapers are either cigarette smokers or ex–smokers of cigarettes, justifies inferring the respiratory parameters of vaping (especially exhaled volume) from the respiratory parameters of smoking reported in the literature (see reviews in Bernstein (2004); Marian et al. (2009), see also Table 3).

3.1.1. Respiratory parameters of smoking

While there is a wide individual diversity in respiratory parameters among smokers, roughly the same three puffing topography patterns identified in section 2.1 for vaping occur in smoking (with tobacco smoke instead of ECA) Higenbottam et al. (1980). As with vaping, the most common cigarette smoking topography is MTL, an expected outcome since most vapers are either ex-smokers or current smokers of cigarettes. While a sizable minority of 10-20 % of vapers (see Section 2.1.2) follow the DLT style, the vast majority of smokers avoid direct lung inhalation because it is too irritant Tobin et al. (1982b) (and is consistently associated with airways narrowing Higenbottam et al. (1980)). In fact, avoidance of the direct lung inhalation of DTL style is very likely an organic response to minimize to a tolerable level the irritant quality of tobacco smoke Higenbottam et al. (1980); Tobin et al. (1982b,a).

Few cigarette smokers and vapers follow a Mouth Puffing topography, but the latter is the preferred pattern among most cigar and tobacco pipe smokers. The physiological differences between Mouth Puffing and MTL patterns was examined by Rodenstein and Stanescu in an observational study Rodenstein and Stănescu (1985) involving exclusive pipe and cigarette smokes,

as well as never smokers. They found that in pipe smokers oral inhalation and nasal breathing remained separate processes in which the oropharyngeal isthmus remained closed (see further discussion on this in Section 3.2) to prevent overt lung inhalation of smoke. However, in cigarette smokers the two processes subsequently interfered with each other once the soft palate and tongue separate to open the oropharyngeal isthmus to allow a deep lung inhalation of the retained smoke bolus in the oropharynx by joint mouth and nose breath inspiration. As a consequence of these differences, most pipe smokers keep a fairly regular breathing pattern similar to that of normal rest breathing with small fluctuations of tidal volume, while cigarette smoking (and most likely MTL and DTL vaping) is characterized by large and irregular tidal volume fluctuations markedly distinct from normal breathing.

Regarding its respiratory parameters, cigarette smoking involves a larger percentage of vital capacity than rest breathing: 20-25 % Bernstein (2004), though low intensity inhalators might use on average only 14 % Tobin et al. (1982a). Again, it is extremely likely that these figures apply at least to MTL vaping). Other parameters such as tidal volume, puff times and volumes obtained in observational studies are listed in Table 2, where we used outcomes from references cited in two comprehensive reviews Bernstein (2004); Marian et al. (2009). The summary of these outcomes is roughly:

- Puff Volume" (volume of the smoke bolus drawn from the cigarette) 20-70 mL,
- Puffing Times (time to draw the smoke bolus from the cigarette) $\sim$ 2 seconds
- Total smoking time lapses (inhalation, breath hold and exhalation) $\sim$ 4 seconds
- Tidal volumes (the volume of the total inhaled/exhaled smoke mixed with air, V_T in table 1) vary widely between 300 and 1500 mL (with some outliers reaching close to 2000 mL), but typically group averages are between 700 and 900 mL

It is worth remarking that puffing times are slightly shorter but roughly comparable to those of MTL vapers, while tidal volumes are 25-30 % larger than rest tidal volumes (400-600 mL), though the measurement of these volumes is subject to at least a 10 % error Herning et al. (1983) and also, not all air drawn with the purpose of inhaling smoke is actually inhaled. Most studies report inhaled volumes, but exhalation volumes are roughly comparable (see Table 2), as smoke is highly diluted in air and its retention barely affects volume measurement.

3.1.2. Suction

As opposed to rest breathing, smoking and vaping involve suction: the inward force needed to draw smoke (or ECA) associated with the negative/positive pressure gradient ΔP generated by the diaphragm driven expansion/contraction of the lungs. Airflow resistance follows from the relation between the flow of air volume $Q = dV/dt$ and this pressure gradient, a relation that can be modeled by the power law Wheatley et al. (1991); Jaeger and Matthys (1968)

$$\Delta P = a\,Q^b, \qquad a, b \text{ constants}, \tag{3}$$

where a, b are determined empirically. This power law can be related to fluid dynamics (see discussion in Jaeger and Matthys (1968)): the constants a and b correlate with fluid density, while the exponents b can be referred to the "classical" flow regimes: $b = 1$ corresponds to laminar flow with Reynolds numbers $Re < 10$ (Pouseuille law), $b = 1.75$ to turbulent flow $Re \sim 10000$

Study authors & reference	**Inhalation/Exhalation Volume (T_V in mL)**	**Puff time/volume** PT seconds, PV mL	**Comments**
US Surgeon Report 1988 See Bernstein Bernstein (2004)	591 (mean), 560 (median) Range 413 – 918	PT 1.8 (mean) PT Range 1.6-2.4 PV 43 (mean) PV Range 21-66	Summary of 32 studies before 1988
Tobin *et al* 1982 Tobin et al. (1982b)	841 ± 517* Natural 748 ± 323** Natural 878 ± 431* Cig Holder 815 ± 376** Cig Holder Range 270-1990 mL		10 subjects Non invasive RIP
Tobin *et al* 1982 Tobin et al. (1982a)	790 ± 450 Group Average 460 ± 130 Rest Tidal Vol Range 270-1970 mL	PT 4.5 ± 1.3 Includes Breath Hold	19 subjects Non invasive RIP
Nil *et al* 1986 Nil et al. (1986)	500 ± 300* Men 600 ± 500** Men 400 ± 300* Women 400 ± 300** Women	PV 42.3 ± 14.5 PV 50.2 ± 16.8 PV 41.4 ± 13.3 PV 47.0 ± 15.8	67 men, 48 women
Woodman *et al* 1986 Woodman et al. (1986)	192-644 Total Inh Smoke 315-919 Total Inh Vol	PT 1.2-2.9	Inert Krypton gas as smoke tracer
Robinson *et al* 1992 Robinson et al. (1992)	828 ± 126 Low Nicotine 845 ± 105 Normal Nicotine		
St. Charles *et al* 2009 Charles et al. (2009)	833 ± 279 Inhaled Vol 897 ± 308 Exhaled Vol 500 ± 148 Rest Tidal Vol	1.82 ± 1.16 Inh Time 2.28 ± 0.87 Exh Time	74 subjects Non invasive RIP without Cig Holder
Marian *et al* 2009 Marian et al. (2009)	702 ± 437* Inh Vol 636 ± 138** Inh Vol 577 ± 329* Exh Vol 655 ± 195** Exh Vol	1.19 ± 0.29*, Inh Time 1.22 ± 0.37**, Inh Time 2.01 ± 0.76*, Exh Time 2.89 ± 0.72*, Exh Time 0.45 ± 0.48*, Breath Hold 0.45 ± 0.57**, Breath Hold PV 44.9 ± 12.3* PV 44.5 ± 10.9**	BAT study 1986 Table 2

Table 2: **Respiratory parameters in cigarette smoking**. The table lists various inhaled/exhaled volumes and associated puff times and volumes. The term "puff time" (PT) denotes the time taken to draw smoke from the cigarette (puffing) with "puff volume" (PV) denoting the drawn volume before it mixes with air. Volumes in the second column refer to the inhaled mixture of smoke and air unless it is explicitly specified that it refers to the exhaled mixture. The symbols ±, * and ** respectively denote standard deviation, high and low TAR yields. RIP refers to Respiratory Inductive Plethysmograph, BAT is British American Tobacco.

(Blasius law) and $b = 2$ is the "orifice" flow characterized by turbulent flow in narrow pipes and containers.

The theoretical connection with fluid mechanics has motivated airflow resistance measurements in the upper respiratory system that yield values around $b = 1.84$ Wheatley et al. (1991); Jaeger and Matthys (1968) for resting oral and nasal breathing. An excellent fit of this power law relation to the classical orifice flow $b = 2$ was found for a conventional cigarette and a two second generation e–cigarettes Sosnowski and Kramek-Romanowska (2016), with the e–cigarettes flow resistance a between 3-4 times larger than the conventional cigarette. As a consequence, given the same suction effort (same ΔP) a conventional cigarette yields a puffing flow Q between 3-4 times larger than the tested e–cigarettes (second generation). However, vapers can compensate the higher flow resistance of ECA and draw relatively large aerosol mass with the same suction effort by puffing for longer times (as shown by topography studies). Also, the laboratory measurements in Sosnowski and Kramek-Romanowska (2016) were conducted under idealized conditions and are very likely to vary among the many e-cigarette devices in natural usage conditions.

A factor that distinguishes cigarette smoking from vaping is that the latter involves suction of ECA through a mouthpiece. However, in most of the studies listed in Table 2 the subjects smoked through cigarette holders that are part of the laboratory instrumentation. This makes the listed outcomes more useful to infer respiratory parameters for vapers, at least for those vaping in the MTL style, since these holders are of similar size and shape as the narrow e–cigarette mouthpieces. Though, usage of cigarette holders does not seem to introduce significant changes in tidal volume, as can be seen by comparing outcomes from studies that used holders with those who did not in Table 2 (we comment further on the effect of mouthpieces in Section 3.2).

Since MTL is the most common topography among smokers and vapers (most of whom are ex-smokers or current smokers), we can assume that MTL style vaping is characterized by qualitatively similar puffing and respiratory parameters to those listed in Table 2. While some smokers inhale without a mouth hold as in DTL style, this does not seem to involve in them a significantly higher tidal volume, most likely because it can be too irritant Higenbottam et al. (1980); Tobin et al. (1982a). The lesser irritant nature of ECA is a plausible explanation for a larger proportion of vapers that can tolerate DTL topography, which means suction of a much larger aerosol mass Soulet et al. (2019); Cahours and Prasad (2018) and thus significantly larger puffing and tidal volumes than in MTL style (made easier by usage of high powered devices). A puff volume of 500 mL can yield under idealized laboratory conditions an inhalation tidal volume close to 3 LT Vas et al. (2015), which justifies the more plausible values listed in Table 1.

3.2. **Mouthpieces, noseclips and the breathing route**

Mouthpieces (MP) and nose-clips (NC) (to block nasal inspiration) are standard instruments in observational studies, not only those aimed at studying droplet emission, but of respiratory patterns and flows in human subjects. Since the results of these studies can serve as appropriate proxy values to infer droplet emission in vaping, it is important to assess the effects of these instruments in respiratory mechanics. For the purpose of the present article, this issue is interesting because ECA is inhaled in e–cigarettes through mouthpieces (though without obstruction of nasal breathing).

3.2.1. Observational data on breathing through mouthpieces and noseclips

Several studies conducted in the 1970's and 1980's Gilbert et al. (1972); Askanazi et al. (1980); Hirsch and Bishop (1982); Douglas et al. (1983); Weissman et al. (1984) have shown

that breathing through MP's and NC' affect all respiratory parameters with respect to unencumbered nose breathing: while tidal volume increases roughly 20 % with respect to its normal rest value of 400-600 mL in all studies, inhalation and exhalation times and respiratory frequency are much less affected. In Weissman et al. (1984) a NC without a MP produces a similar increase of tidal volume but also significant increase of inhalation times (15 %) and exhalation times (22 %). Two of the studies Gilbert et al. (1972); Askanazi et al. (1980); Weissman et al. (1984) were conducted on subjects in supine position, but different body positions only produce minor variation of respiratory parameters Kera and Maruyama (2005).

Besides possible reasons like the psychological sensorial stimulation of receptors by colder air in mouth inspiration and the stress of breathing through instruments, another possible explanation for the observed change in respiratory parameters of MP's is the change of airflow resistance, for example: a 70–90 % reduction Weissman et al. (1984) brought by the large added mouthpiece dead space (up to 80 mL), while the larger airflow resistance from the standard 17 mm to a narrower 9 mm MP (closer in size to mouthpieces used in vaping) reduced the increase of tidal volume to 11 % and inhalation/exhalation times to 9 % Weissman et al. (1984). Therefore, the MP's of e-cigarettes should not produce significant modifications of respiratory parameters.

The relation between airflow resistance and MP diameter follows from comparing fluid flow in the MP with that along a Venturi-meter tube in which the Reynolds number is $Re = 4\rho Q/(\pi \mu d)$, with ρ, μ the fluid density and dynamical viscosity and d the tube diameter. The pressure gradient vs flow Q is given by (3), which for the expected turbulent flow in a MP (negligible effect of μ) can be expressed in terms of ρ and d (the MP diameter) qualitatively as $\Delta P \propto (\rho Q^2)/d^4$ (see Jaeger and Matthys (1968)). Hence, in a comparison of two e–cigarette MP's the same suction effort $(\Delta P)_2 = (\Delta P)_1$ yields for the MP with larger diameter ($d_2 > d_1$) a larger flow $Q_2/Q_1 \propto (d_2/d_1)^4$.

3.2.2. Effects of the breathing route

In the studies discussed above there was no separation between usage of instruments (MP & NC) and oral breathing. Rodenstein, Mercenier and Stanescu Rodenstein et al. (1985) conducted several experiments with 14 healthy subjects with the aim of looking separately at the effects of MP's and a NC's. Their results show that breathing through a MP without a NC (with and without instructing the subjects on how to breath) practically keeps all respiratory parameters identical to those of normal nasal breathing with closed mouth: resting tidal volume barely changed from 533 ± 253 to 559 ± 284 mL, breathing cycle (time for inspiration and expiration) practically remained the same at 4.8 ± 2.3 and 4.9 ± 1.8 seconds. They observed that 9 of 14 subjects breathed in a normal manner even if their mouth was connected to a MP. However, they observed qualitatively the same changes as Gilbert et al. (1972); Askanazi et al. (1980); Hirsch and Bishop (1982); Douglas et al. (1983); Weissman et al. (1984) with subjects breathing through an MP plus NC: tidal volume increased to 699 ± 415 mL and inhalation/exhalation time to 5.5 seconds.

The main result of Rodenstein et al is that changes of respiratory parameters (rough 20 % and 10 % increase of tidal volume and inhalation/exhalation cycle) are entirely due to the forced oral breathing induced by the NC, in fact, nose occlusion is not even necessary to produce these changes: it is sufficient to simply instruct the subjects to breath through the mouth to observe an increase the tidal volume by a similar proportion as with the use of a NC: from 456 ± 142 to 571 ± 199 mL, though inhalation/exhalation times and other parameters remain almost the same (likely because of breathing without instrumentation).

The physiology behind the effects of the breathing route is similar to the one discussed in the study of pipe and cigarette smokers Rodenstein and Stănescu (1985): changes of respiratory

parameters depend on the degree with which subjects are able to maintain air flowing through the nose. These parameters exhibit minor variation as long as this air flow is not occluded and the oropharyngeal isthmus remains closed. The parameters change significantly when nose occlusion separates the soft palate and the tongue and opens the oropharyngeal isthmus to allow air to flow entirely through the mouth. However, after the initial puffing, air flows through both nose and mouth in smoking and vaping (except the Mouth Puffing style), with the soft palate closing and rising enough to control the oral or nasal flow.

3.3. **Likely characteristics of respiratory droplets carried by ECA**

The discussion in the previous sections has allowed us to infer the characteristics and parameters of the respiratory mechanics of vaping. We need now to identify among respiratory processes the ones that most closely fit these parameters in order to use their available experimental data to infer the capacity of vaping for respiratory droplets emission.

3.3.1. The right respiratory proxy: mouth breathing

Given the fact that exhaled ECA is a single phase flow (SFF) system (see section 2.3), a good criterion to relate vaping to other respiratory processes is the comparison between its fluid exhalation velocity U_0 and measured analogous velocities in other respiratory processes.

The exhalation velocity U_0 can be roughly inferred qualitatively by considering an exhaled tidal volume of fluid flowing through the respiratory tracts. Considering the respiratory parameters discussed in the previous sections (summarized in Table 1) we can use the simple approximate formula

$$U_0 \approx \frac{V_T}{t_{\text{exh}} A}, \tag{4}$$

where V_T is the exhalation tidal volume (in cm^3), t_{exh} is the exhalation time in seconds and A is the combined mouth and nose area (in cm^2), as the fluid carrier of both ECA and tobacco smoke is exhaled through the mouth and nose. From the values listed in Tables 1 and 2 we have:

- MTL vaping and smoking: $V_T = 300 - 1500$ mL and $t_{\text{exh}} = 2 - 3$ sec., while values for the combined mouth/nose area has been measured between $A = 2 - 3\,\text{cm}^2$ Gupta et al. (2010).
- DTL Vaping: $V_T = 1000 - 3000$ mL with $t_{\text{exh}} \approx 3 - 4$ sec. and $A \approx 3\,\text{cm}^2$. Given the large amount of exhaled fluid we assume longer exhalation times and larger mouth opening area.

From the combination of the parameter values mentioned above we have

$$U_0 \approx 30 - 300\,\frac{\text{cm}}{\text{s}} \quad \text{MTL} \qquad U_0 \approx 150 - 400\,\frac{\text{cm}}{\text{s}} \quad \text{DTL}, \tag{5}$$

which indicates that mouth breathing is the appropriate respiratory proxy for MTL vaping and cigarette smoking, as well as the less intense DTL regime (up to 300 cm/sec), since these estimated exhalation velocities are well within the range of those of exhaled breath in mouth breathing without nose occlusion by NC's Xu (2018); Xu et al. (2015, 2017), which have been estimated and measured by various techniques (including Schlieren photography). Exhalation velocities in the most intense DTL vaping regime approach in their upper end the velocities of vocalizing but fall short of those of coughing and sneezing. As a reference, measurements of U_0 using Particle Image Velocimetry resulted in averages of 3.9 m/s for speaking and 11.7 m/s for coughing Chao et al. (2009) (measurements in Zhu et al. (2006) resulted in 6-22 m/s with average 11.2 m/s for coughing), while 35 m/s has been estimated for sneezing Chen and Zhao (2010); Wei and Li (2016); Scharfman et al. (2016).

3.3.2. Data on droplet emission from mouth breathing

There is an extensive literature on respiratory droplets emitted by mouth breathing at different levels of lung capacity, including rest tidal volume breathing (< 20 % of vital capacity). We list a selection of these studies in Table 3, as they are the ones that can serve as proxies for vaping and smoking (at least MTL style). In practically all the listed studies subjects breathed through MP's (mouthpieces) and NC's (noseclips), which as discussed in section 3.2, involves occlusion of nasal air flow that implies a slightly modified mechanics and about 20 % larger tidal volume with respect to normal unencumbered breathing.

The fact that emitted respiratory droplets in tidal volumes close to rest breathing are overwhelmingly in the submicron range (as shown by Table 3) implies a very rapid evaporation (0.01 sec) that in practice can be considered as instantaneous, with the emitted droplets being overwhelmingly desiccated droplet nuclei made of salt crystals and lypoproteins and being about roughly half Nicas et al. (2005) their original diameter. The exhaled breath will also contain some larger particles $d_p \sim 1 - 3\,\mu$m that evaporate in timescales of 0.1 sec so that (given the exhalation velocities in (5)) they become desiccated nuclei at horizontal distances of 10-30 cm. As a consequence, relative humidity bears negligible influence on the evolution of the bulk of emitted droplets.

While some of the studies in Table 3 were motivated by investigating droplet emission in the context of airborne pathogen contagion Papineni and Rosenthal (1997); Fabian et al. (2011); Wurie et al. (2013); Asadi et al. (2019), the motivation of others Johnson and Morawska (2009); Morawska et al. (2009); Almstrand et al. (2010); Holmgren et al. (2010); Schwarz et al. (2010, 2015) is to probe various mechanisms of droplet formation (see comprehensive discussion and reviews in Wei and Li (2016); Bake et al. (2019); Haslbeck et al. (2010)), specifically the airway reopening hypothesis of small peripheral airways that normally close following a deep expiration, which was further tested by computerized modeling Haslbeck et al. (2010) that simulated this mechanism of particle formation by rupture of surfactant films involving surface tension. The mechanism was probed in Johnson and Morawska (2009) by showing that concentrations of exhaled particles significantly increase with breathing intensities higher than rest tidal volume, but also for fast exhalations but not fast inhalation, while droplet numbers increased up to two orders of magnitude: from $\sim$ 230/LT in tidal volume (0.7 Lt) to over 1200/LT in a breathing maneuver from fractional residual capacity to total lung capacity Almstrand et al. (2010).

The difference in droplet formation between breathing and speaking was examined in Johnson et al. (2011): normal and deep tidal breathing produced submicron distributions related to those of other studies probing the airway reopening mechanism, while speech and cough produced larger diameter modes ($\sim 1\,\mu$m) with particle formation associated with vocal cord vibrations and aerosolization in the laryngeal region. A third mode of median diameters of 200μm was associated with the presence of saliva between the epiglottis and the lips.

Breath holding between inspiration and expiration were found in Johnson and Morawska (2009) to significantly reduce concentrations of exhaled droplets in proportion to the breath hold time. The same outcome resulted in Holmgren et al. (2013) for inspiration to total lung capacity, but droplet numbers increased when the breath hold occurs before inspiration. These outcomes fit predicted effects of gravitational settling in the alveolar region. Since observations in Johnson and Morawska (2009); Holmgren et al. (2013) involved breathing intensity well above tidal volume up to total vital capacity, it is not possible to compare them quantitatively with the breath hold of the MTL style. However, gravitational settling of larger droplets must also occur in the bucal cavity under normal vaping conditions Asgharian et al. (2018), so it is reasonable to as-

sume that reduction of exhaled droplet numbers should also occur at lower intensity in MTL style vaping.

Methods II: Assessing exposure

4. Hydrodynamical modeling of direct exposure

In the previous sections we have inferred the submicron characteristics and rate of emission of respiratory droplets expected to be carried by exhaled ECA. We need to estimate now how far can these respiratory droplets be carried to evaluate the distance for direct exposure of bystanders to pathogens potentially carried by these droplets

Exhaled ECA is injected into surrounding air a given horizontal distance roughly in the direction of the exhaled flow. Since it involes a finite fluid mass of a SFF aerosol during a finite injection time (exhalation time), the appropriate dynamical model for it is a turbulent puff with a starting momentum dominated jet that lasts while the fluid injection is on Pope (2001); Rajaratnam (1976); Abani and Reitz (2007); Abraham (1996); Ghaem-Maghami (2006); Ghaem-Maghami and Johari (2010); Sangras et al. (2002, 2003). A schematic description of this system is furnished by Figure 3. We will not be concerned with the few larger particles (diameters $d \sim 1-5\mu$m and over) that initially follow the fluid stream but (depending on their size) exit the main flow to follow ballistic trajectories until they either deposit on surfaces, settle on the ground or evaporate Wei and Li (2016); Bourouiba et al. (2014).

Given the distance and time dispersion scales ($<$ 3 meters and $<$ 2-3 minutes) we can approximate the ECA as an airflow at constant atmospheric pressure, air density and dynamical viscosity ρ_a and μ. For a jet source (vaper's mouth) approximated as an orifice of $1.5-3\,\mathrm{cm}^2$ area Gupta et al. (2010) (diameter d_0 =1.25-1.75 cm) and initial velocities U_0 given by (5), exhalation Reynolds numbers $Re = (\rho/\mu)U_0 d_0 = 600-4400$ are in the transition between laminar and turbulent, values well below the high Reynolds numbers expected near a jet source Pope (2001); Rajaratnam (1976), but we are mostly concerned with the jet evolution and displacement (penetration) along horizontal distances $z \gg d_0$. Other parameters to consider are the injection time $t_{\mathrm{exh}} = 2-5$ seconds and a temperature gradient from exhalation (initial) $T = 30^\circ - 35^\circ$ C (mouth temperature) into an assumed $T = 20^\circ$ C for the surrounding air. For such values and scales the starting jet can be regarded as isothermal with thermal buoyancy becoming relevant only in the puff stage Ghaem-Maghami (2006); Ghaem-Maghami and Johari (2010). It is well known that steady and unsteady jet/puff systems can be well approximated by analytic models that assume axial symmetry and a self similar profile for the average centerline and radial components of the velocity field in cylindrical coordinates $\vec{U} = [U_z, U_r, U_\phi]$ Pope (2001); Rajaratnam (1976); Morton et al. (1994); Shin et al. (2017) (see figure 3)

$$U_z = U_c(t)\, f(\eta), \quad U_r = U_c(t)\, g(\eta), \quad U_\phi = 0, \tag{6}$$

where f, g are empiric Gaussian or polynomial functions of the self similar variable $\eta = r/z$ and the centerline velocity is $U_c = U_z$ for $r = 0$ along the z axis, hence $f(\eta)$, $g(\eta)$ must satisfy $U_z = U_c$ and $U_r = 0$ at $r = 0$ (see examples in Wei and Li (2016); Pope (2001); Rajaratnam (1976); Abani and Reitz (2007); Abraham (1996); Ghaem-Maghami (2006); Ghaem-Maghami and Johari (2010); Sangras et al. (2002, 2003)). An axially symmetric self similar jet/puff system fulfills the conservation of linear specific momentum $Q = V\,U_c$ (puff) and force $\dot{Q} = (d/dt)(V\,U_c)$ (jet) where V is the penetration volume Pope (2001); Sangras et al. (2002,

Study authors & reference	**Droplet numbers, density & diameters**	**Subjects**	**Comments & Technique**
Pepineni–Rosenthal 1996 Papineni and Rosenthal (1997)	Mean $N_p = 12.5$/L, ($< 1\mu$m) Mean $N_p = 1.9$/L, ($> 1\mu$m)	5 healthy	Table 2 OPC, EM
Johnson–Morawska 2008 Johnson and Morawska (2009)	$n_p < 0.25/\text{cm}^3$ (V_T) up to $n_p = 2.5/\text{cm}^3$ (deep)	17 healthy ages 19–60	Figures 3 & 7. BH decreases droplet numbers APS
Morawska *et al* 2009 Morawska et al. (2009)	Mean $N_p = 98$/L Mean $d_p = 0.8\,\mu$m	15 healthy ages < 35	nose inhalation & mouth exhalation APS
Armstrand *et al* 2010 Almstrand et al. (2010)	$N_p = 230$/L, $(18 - 1000)/L$ $d_p = 0.3 - 0.4\,\mu$m 98% $d_p < 1.0\,\mu$m	10 healthy ages 29–69	Tidal Volume Tables 2 & 3 OPC
Holmgren *et al* 2010 Holmgren et al. (2010)	Median $n_p = 3.1\,(0.6 - 82)/\text{cm}^3$ $\bar{d}_p = 0.07\,\mu$m $V_{\text{ex}} = 351 - 1701\,\text{cm}^3$	16 healthy	Tables 3 & 4 Two super emitters SMPS
Schwarz *et al* 2010 Schwarz et al. (2010)	$N_p \approx 10 - 50$/exh Median $d_p = 0.28\,\mu$m	21 healthy (4 smokers)	Close to V_T $V_T/V_C \approx 0.2$ CNC
Fabian *et al* 2011 Fabian et al. (2011)	GMean $N_p = 7.4$/L LE GMean $N_p = 3500$/L HE 82% $d_p = 0.3 - 0.5\,\mu$m	19 subjects (7 asthmatic)	4 HE Table 1 OPC
Wurie *et al* 2014 Wurie et al. (2013)	Median $N_p = 38.3\,(3.3 - 1456)$/L 90% $N_p < 150$/L, LE 99.9% $d_p < 1.0\,\mu$m 75% $d_p < 0.5\,\mu$m	79 healthy (14 asthmatic)	4-19% high emitters follow up of subjects OPC
Schwarz *et al* 2015 Schwarz et al. (2015)	$N_p \approx 10$/exh LE up tp $N_p \approx 1000$/exh HE Median $d_p = 0.3\,\mu$m	29 healthy (13 smokers) 28 COPD 10 asthmatic	Figures 2 & 4 Close to V_T $V_T/V_C \approx 0.2$ CNC
Asadi *et al* 2019 Asadi et al. (2019)	$N_p \approx 1$/sec $d_p = 0.75 - 1.0\,\mu$m $n_p < 0.1/\text{cm}^3$	48 healthy age 18-45 10 asthmatic	Figure 5 much larger in speech than in breathing APS

Table 3: **Droplet emissions for mouth breathing and tidal volume**. The symbols N_p and n_p stand for droplet number per exhalation and average droplet number density (cm^{-3}). LE, HE, BH, L, and exh are Low emitters, High Emitters, Breath Hold, litter and exhalation. The acronyms OPC, EM, APS, SMPS, CNC stand for Optical Particle Counter, Electron Microscopy, Aerodynamic Particle Sizer, Scanning Mobility Particle Sizer, Condensation Nucleus Counter. The subjects in all studies (save possibly Johnson and Morawska (2009)) breathed through a mouthpiece wearing a noseclip.

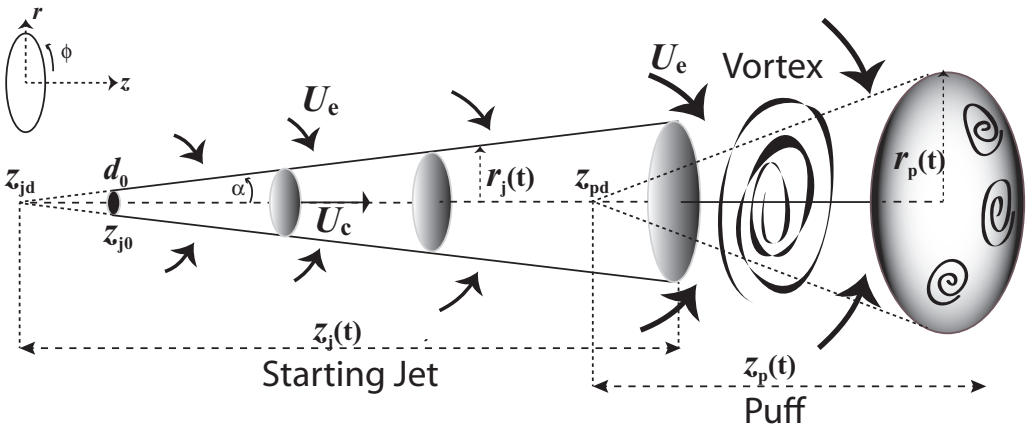

Figure 2: Puff and initial Jet with axial symmetry. The stating jet is propelled by linear momentum parallel to the centerline velocity U_c, the arrows above and below represent the entrainment velocity mixing surrounding air with the carrier fluid. As the fluid injection terminates (end of exhalation), the entrained air makes about 40 % of the fluid mass making the the transition into a ellipsoidal puff through highly turbulent vortex structures. At this point the puff is likely to disperse rapidly as horizontal displacement velocities are comparable to velocity fluctuations characterizing high turbulence and thermal buoyancy.

2003), hence $Q = Q_0$, $\dot{Q} = \dot{Q}_0$ for an initial time $t = t_0$. The stream wise centerline penetration distance and velocity for the jet and puff stages can be given by Sangras et al. (2002, 2003):

$$\text{Starting Jet} \quad z_j(t) - z_{j0} = C_{jz}\left(\dot{Q}_0\, U_0\right)^{1/4}(t - t_{j0})^{1/2}, \qquad r_j(t) = C_{jr}\, z_j(t), \tag{7}$$

$$U_{cj} = \frac{dz_j}{dt} = \frac{C_{jz}^2\,(\dot{Q}_0 U_0)^{1/2}}{2\,(z - z_{j0})}, \tag{8}$$

$$\text{Puff Stage} \quad z_p(t) - z_{pd} = C_{pz}\,(Q_0\, U_0)^{1/4}\,(t - t_{p0})^{1/4}, \qquad r_p(t) = C_{pr}\, z_p(t), \tag{9}$$

$$U_{cp} = \frac{dz_p}{dt} = \frac{C_{pz}^4\, Q_0 U_0}{4\,(z - z_{pd})^3}, \tag{10}$$

where the constants $C_{jz}, C_{jr}, C_{pz}, C_{pr}$ are empirically determined, and z_{j0} is the z coordinate value of the ejection orifice and z_{pd} is the virtual origins of the puff (see Figure 2), which is an appropriate parameter to separate the starting jet and puff stages though it lies within the starting jet region (see detailed explanation in Sangras et al. (2002)). For the axial geometry of the jet/puff system under consideration we have $Q_0 U_0 = \pi d_0^2 U_0/(8C_{pr}^2)$ and $\dot{Q}_0 U_0 = (3\pi/4) d_0^2\, U_0^2$. Following Sangras et al. (2002, 2003), we will choose the following numerical values for the constants in (7)–(10):

$$C_{jz} = 2.8, \quad C_{jr} = 0.15, \quad z_{j0} = d_0/(2C_{jr}), \tag{11}$$

$$C_{pz} = 2.6, \quad C_{jr} = 0.17, \quad z_{pd} = z_j(t_{\text{exh}}) - 8.5 d_0, \tag{12}$$

where the time t_{pd} and position of the puff virtual origin z_{pd} is determined numerically from (7) by the condition $z_j(t_{pd}) = z_{pd}$ Sangras et al. (2002, 2003). Many vapers exhale at a downward angle typically $\gamma \sim 30$ degrees, thus reducing the horizontal penetration of the starting jet given by (7) roughly as $z_j \cos\gamma$. From the dynamical equations (7)–(10) with the parameter values in

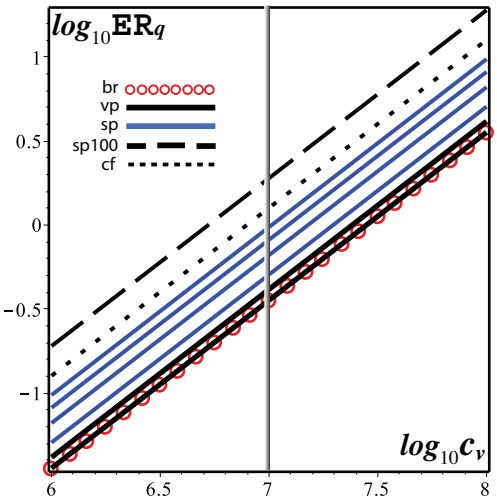

Figure 3: **Quanta emission rates.** The curves display ER_q (quanta/hour) as a function of viral load c_v (RNA copies/mL) for various expiratory activities: rest breathing (br), low and high intensity vaping (vp), speaking (bottom to top) 10, 20, 30, 40 % of the hour (sp), coughing (cf) and speaking 100 % of the time (sp100). Numerical values of ER_q for $c_v = 10^7$ RNA copies/mL (vertical line) are listed and discussed in the text. The ratios between these activities and rest breathing (taken as the case control scenario) is displayed in figure 7.

(11)–(12) we display in section 7.3 the horizontal distance and jet/puff velocities characterizing direct exposure.

5. Risk model of contagion

We have evaluated the distance spread in which exhaled ECA can produce direct contagion by horizontally spreading overwhelmingly submicron respiratory droplets, which once reaching the turbulent puff regime remain buoyant for hours, possibly producing indirect contagion as they are carried by indoor air currents several meters (see comprehensive analysis in Vuorinen et al. (2020)). So far we have considered generic respiratory droplets without reference to a specific pathogen/disease and have not evaluated infection risks of exposed susceptible individuals. We undertake now this evaluation, referring specifically to the available information on the parameters of the SARS-CoV-2 virus, assuming as well that emitted respiratory droplets or droplet nuclei potentially carrying this virus have been dispersed uniformly throughout a given indoor micro-environment.

The most important feature that fully characterizes exposure risks from vaping expirations is the significant shortening of exposure time because of their intermittent and episodic nature: an infectious vaper (symptomatic or not) would emit respiratory droplets only while vaping (120-200 daily exhalations Dautzenberg and Bricard (2015); Cahours and Prasad (2018)), whereas the same vaper will emit respiratory droplets continuously just by normal rest breathing (17,000–29,000 daily exhalations for 12-20 breaths per minute for healthy adults).

5.1. *Infective quanta*

To evaluate indirect exposure risks from vaping we simplify and adapt the analytic risk model of Buonanno, Morawska and Stabile (hereafter BMS) Buonanno et al. (2020a) who have examined the potential SARS-CoV-2 virus transmission in various indoor micro-environments (see also their previous paper Buonanno et al. (2020b)). BMS develop this model by means of Montecarlo simulations in which variability of droplet emission rates and exposure parameters is described by suitable probability distributions. Our approach is to assume median values for these variables (50 percentiles) of these distributions, similar to their approach in their previous paper Buonanno et al. (2020b). This is justified because our aim is to evaluate the risks from indoor COVID-19 transmission from vaping, speaking and coughing (all episodic or intermittent expirations) in comparison with what can be denoted as a "control case" scenario of risks in a space were the infectious vaper is only rest breathing (a continuous expiration). We are not aiming at providing a full comprehensive risk analysis for each respiratory activity separately under more realistic conditions (something that would justify a full separate study in itself).

BSM consider the notion of an infective "quantum": the dose of airborne respiratory droplet nuclei necessary to infect 63 % of exposed susceptible individuals. They introduce the "quantum emission rate" $\mathtt{ER}_q$ (emitted quanta per hour) for various respiratory expirations

$$\mathtt{ER}_q = \frac{c_v}{c_{\mathrm{RNA}}\, c_{\mathrm{PFU}}} \times f_{\mathrm{br}}\, V_T\, C_d, \tag{13}$$

where c_v is the viral load (RNA copies/mL) in the sputum of a SARS-CoV-2 infected person (symptomatic or not), c_{RNA} is the number of RNA copies per PFU (plaque forming unit) needed to generate infection and c_{PFU} is quanta-to-PFU conversion parameter, f_{br} is the number of breaths per hour and V_T the tidal exhaled volume, C_d is the droplet volume concentration (in $\mathrm{mL/m^3}$, hence $C_d\, V_T$ is the total volume of exhaled droplets in mL). BMS define the product "$IR = V_T \times f_{\mathrm{br}}$" as an "inhalation rate", but it is really an exhalation rate expressible in units $\mathrm{m^3/h}$.

For the infection parameters BMS consider values that have emerged from recent data: $c_v = 10^7$ RNA copies/mL (average in the range $10^3 - 10^{11}$), $c_{\mathrm{RNA}} = 1.3 \times 10^2$ RNA copies/PFU and $c_{\mathrm{PFU}} = 2.1 \times 10^2$ PFU/quanta. For the droplet volume concentration they take as reference an experimental value that incorporated dehydration effects in droplets associated with loud speech Stadnytskyi et al. (2020), then using experimental data from Morawska et al Morawska et al. (2009) to scale this reference to other respiratory expirations, leading to the following values (in $\mathrm{mL/m^3}$)

$$C_d = 2 \times 10^{-2} \text{ (loud speech)}, \quad 6 \times 10^{-3} \text{ (normal speech)}, \quad 2 \times 10^{-3} \text{ (rest breathing)}, \tag{14}$$

In order to fit vaping expirations into these values we need to make some assumptions on the involved parameters, besides considering the effects on exposure from the time duration of expiratory activities. In particular, we need to evaluate their mean quanta emission rate *only* in the times when they occur and compare with the rates of normal rest breathing (which takes place all the time). To simplify matters, we assume that c_v, c_{I} and $f_{(\mathrm{br})}$ are largely unaffected by the timing of these expiratory activities. We have then

- **Low intensity MTL Vaping**. A vaper breathes $N_{(\mathrm{tot})}$ times in (say) one hour and of these breaths $N_{(\mathrm{vp})}$ coincide with vaping expirations (puffs), the expression for $\mathtt{ER}_q$ in (13) must

be modified as

$$\mathrm{ER}_{q(\mathrm{vp})} = \frac{c_v\, f_{\mathrm{br}}}{c_{\mathrm{RNA}} + c_{\mathrm{PFU}}} \left[\frac{N_{(\mathrm{vp})}}{N_{(\mathrm{tot})}} V_{T\,(\mathrm{vp})}\, C_{d(\mathrm{vp})} + \left(1 - \frac{N_{(\mathrm{vp})}}{N_{(\mathrm{tot})}}\right) V_{T\,(\mathrm{br})}\, C_{d(\mathrm{br})} \right], \tag{15}$$

where $N_{(\mathrm{vp})}$ $N_{(\mathrm{tot})}$ are the number of vaping puffs and total number of breaths per hour, $V_{T(\mathrm{br})}$ $V_{T(\mathrm{vp})}$ and $C_{d(\mathrm{vp})}$, $C_{i(\mathrm{br})}$ are the tidal volumes and droplet volume concentration for vaping and rest breathing. For low intensity MTL vaping we assume a tidal volume of $V_T = 750\,\mathrm{cm}^3$ supported by inference from data discussed in previous sections, while for droplet volume concentration we assume $C_d = 3\times10^{-3}\,\mathrm{mL/m}^3$, a plausible value denoting emissions slightly above rest breathing but below normal speech in (14), fitting the 'whispered counting' data of Morawska et al. (2009). For the number of breaths we can take the average values of 160 daily puffs in a 16 hour journey Dautzenberg and Bricard (2015); Cahours and Prasad (2018) and breathing frequency of $f_{(\mathrm{br})} = 16/\mathrm{min}$ (in the range 12-20), so that $N_{(\mathrm{tot})} = 960$ breaths/h and $N_{(\mathrm{vp})} = 10$ breaths/h.

- **High intensity DTL vaping**. We assume $V_T = 2000\,\mathrm{cm}^3$ as an average tidal volume. However, there is ambiguity in inferring a value for droplet volume concentration because of insufficient data on how much the larger tidal volume and deeper inhalation of DTL vaping can modify respiratory droplet numbers and diameters. As mentioned in section 2.2, higher powered devices associated with DTL vaping tend to increase ECA droplet sizes and diameters Lechasseur et al. (2019); Floyd et al. (2018) but it is not certain if this applies to respiratory droplets. However, as mentioned in section 3.3, speech involves droplet generating mechanisms that are distinct from those of breathing Asadi et al. (2019); Morawska et al. (2009); Johnson et al. (2011), resulting in higher rate of droplet emission even with a tidal volume only slightly larger than the breathing rest value of $400-600\,\mathrm{cm}^3$ Bailey and Hoit (2002); Hoshiko (1965). Thus, we have two plausible options to account for a higher total volume of exhaled droplets $\mathcal{V}_d = V_T\, C_d$: it may follow simply from a larger V_T with the same value $C_d = 3\times10^{-3}\,\mathrm{mL/m}^3$ of low intensity vaping, or we might assume the larger value of C_d for normal speech in (14). Instead of choosing one option, we will keep the continuous range of $C_d = 3-6\times10^{-3}\,\mathrm{mL/m}^3$. Regarding the number of breaths we can assume the same values as low intensity vaping: $N_{(\mathrm{tot})} = 960$ breaths/h and $N_{(\mathrm{vp})} = 10$ breaths/h.

- **Normal speech**. The equation for ER_q in (13) needs to be modified in a similar way as (15), replacing the droplet volume concentration C_d with the value for normal speech in (14) and we take as tidal volume the value $V_T = 600\,\mathrm{cm}^3$, roughly 10 % larger than the average rest value Bailey and Hoit (2002); Hoshiko (1965). To incorporate the timing we replace $N_{(\mathrm{vp})}$ with a number count of breaths coinciding with a given percentage of an hour interval spent on continuously speaking in a given indoor environmant. For 5, 10, 20, 30, 40 % of the hour (960 total breaths) we have $N_{(\mathrm{sp})} = 48, 96, 192, 288, 384$ breaths/h.

- **Coughing**. The emission data from coughing in Morawska et al. (2009) is comparable to that of 'unmodulated vocalization' (repeating the vowel "aahh"). Hence, we can use (15) with the value for droplet concentration volume of loud speaking in (14) as a proxy for coughing, while for coughing tidal volume we have $V_T = 1400\,\mathrm{cm}^3$ Gupta et al. (2009). Assuming a cough every 2 and 3 minutes, $N_{(\mathrm{vp})}$ is replaced by $N_{(\mathrm{cf})} = 20, 30$.

Considering the plausible assumptions stated above, we display in figure 3 the logarithmic plots of quanta emission rate ER_q from an infectious individual as a function of viral load c_v, for rest

breathing, low and high intensity vaping, speaking for 10 %, 20 %, 30 % and 100 % of the time, as well as coughing every 2 and 3 minutes. The numerical values of $\mathtt{ER}_q$ in quanta per hour for $c_v = 10^7$ RNA copies/mL are

$$\begin{aligned} \mathtt{ER}_{q(\mathtt{br})} &= 0.3416, \quad \mathtt{ER}_{q(\mathtt{vpL})} = 0.3562, \quad \mathtt{ER}_{q(\mathtt{vpH})} = 0.3727 - 0.4139, \\ \mathtt{ER}_{q(\mathtt{sp10})} &= 0.5063, \quad \mathtt{ER}_{q(\mathtt{sp20})} = 0.6610, \quad \mathtt{ER}_{q(\mathtt{sp30})} = 0.8158, \\ \mathtt{ER}_{q(\mathtt{sp40})} &= 0.9705, \quad \mathtt{ER}_{q(\mathtt{cf})} = 1.2637, \quad \mathtt{ER}_{q(\mathtt{sp100})} = 1.8216, \end{aligned} \tag{16}$$

where the symbols `br`, `vpL`, `vpH`, `sp10`, `sp20`, `sp30`, `sp40`, `sp100` and `cf` respectively denote breathing, vaping low and high intensity, speaking 10, 20, 30, 40, 100% of the hour and coughing 30 times. Notice that for low and high intensity vaping $\mathtt{ER}_q$ is very close to the control case of rest breathing (almost indistinguishable for low intensity vaping), while even speaking 10 % of the hour (6 minutes) yields a larger $\mathtt{ER}_q$ value than the upper end of high intensity vaping. Also, normal speech for a full hour (not uncommon) produces a higher quanta emission than coughing 30 times

5.2. Exponential dose-response risk model

In order to evaluate a time dependent risk for expiratory activities that incorporates quanta emission rates and indoor environment variables, BSM consider the "dose response exponential model" given in terms of the the density of the quanta $n(t)$ in units quanta/m^3 under the assumption that $n(0) = 0$ (no exposure at initial time $t = 0$)

$$R = 1 - \exp\left[-\mathtt{IR} \int_0^T n(t)\, dt\right] = 1 - \exp\left[-\frac{\mathtt{IR}\,[\mathtt{ER}_q\, N\, T - n(T)\, V]}{\mathtt{IVVR}\, V}\right], \tag{17}$$

$$n(t) = \frac{\mathtt{ER}_q\, N}{\mathtt{IVVR}\, V}\left[1 - \exp(-\mathtt{IVVR}\, t)\right], \tag{18}$$

where V is the volume (m^3) of the indoor micro-environment, N is the number of exposed susceptible individuals, $\mathtt{IR}$ is the inhalation rate (m$^3/h$) of these individuals and $\mathtt{IVVR}$ is the infectious virus removal rate, which which BMS take as the sum of three factors: $\mathtt{IVVR} = \mathtt{AER} + \kappa + \lambda$, where $\mathtt{AER}$ is the ventilation air exchange rate, κ is the particle deposition on surfaces and λ is the virus inactivation (all of these quantities given as h^{-1}).

We evaluate in section 7.4 the risk R for vaping exhalations and other respiratory activities, aiming at the evaluation of their relative risk with respect to the control state of continuous breathing, assuming a home and restaurant scenarios with natural and mechanical ventilation.

6. Disinfectant properties of ECA

As mentioned in the Introduction, respiratory droplets potentially carrying the SARS-CoV-2 virus that are exhaled by vapers are not really "airborne" but "ECA–borne", *i.e.* they are carried by a completely different chemical environment relative to air diluted plain exhaled breath condensates. It is thus important to discuss the potential effect on the pathogens by known mechanisms of disinfection of glycols such as propylene glycol (PG) and Glycerol or Vegetable Glycerine (VG), which are the main co-solvents used in the process of generation of ECA (and are also the main ingredients in the nicotine containing e-liquids).

Both PG and VG are organic compounds of the family of polyfunctional alcohols, commonly used as drug solubilizers in topical, oral, inhaled, nasal, optical and intravenous medications, as

well as water-miscible co-solvents that provide both antimicrobial properties and an increase of the overall stability of many liquid pharmaceutical forms EMA (2017); Rowe et al. (2009); USE (1980); De Spiegeleer et al. (2006). Since both PG and VG are known hygroscopic compounds, they have been used to induce or sustain desiccation in gases Shoaib et al. (2016), and conversely in liquid formulations to preserve hydration in several applications as humectants Pub (2000a,b).

The numerous applications of PG include

- Antiseptic: provides antimicrobial activity similar to that of ethanol Rowe et al. (2009).
- As an active ingredient it has been used in air sanitization USE (1980), product preservation De Spiegeleer et al. (2006)
- Hard surface disinfection against bacteria, fungi and viruses, while as a food ingredient PG has been used as co-solvent, humectant, rheological modifier Pub (2000a).
- Preservative demonstrating complete bactericidal effects at aqueous concentrations of 25 %.

Regarding VG (see Pub (2000b)), it is also known for its antibacterial Nalawade et al. (2015) and antiviral properties Cameron et al. (2000) and is used in several pharmaceutical, cosmetic and food applications due to its relative safety, sweet taste, unique humectant properties (more effective than PG because of its larger viscosity Pub (2000b))

The fundamental mechanisms governing antimicrobial and viral inactivation of VG and PG are still not fully understood, based on the increased efficacy in the presence of water and the dependence of the relative humidity in gases, and water activity in solids and liquids, it is generally believed that these agents can induce microbial membrane damage by dehydration, osmotic effects, phospholipidic membrane and enveloped capsid disarrays caused by hydrophobic-hydrophilic surface alterations, coagulation and denaturation of membrane proteins Kinnunen and Koskela (1991); Puck (1947a).

The aerial disinfection can be initially attributed to the reduction of water and desiccant activity that VG and PG and other glycols have in aqueous solutions and water-containing vapor systems Puck (1947b), glycols after condensation can nucleate by adsorption around aqueous bio droplets driven by the electrostatic attraction that they have towards the water and proteins present in these particles, the intensity of the H-OH hydrogen bonding that both PG, VG and other glycols manifest with water in heterogeneous water polyphase systems also facilitate the reduction of water activity, which can subsequently reduce the viability of these microorganisms suspended as aerosols Marcolli and Peter (2005).

The bactericidal effect of glycols in vapours has been studied since 1928 Puck (1947b,a); Puck et al. (1943); Mather and McClure (1945). During the 1930's and 1940's Puck and Robertson studied the bactericidal and virucidal effects of glycols, particularly PG, acting on several vapor-water systems with suspended microorganisms. As explained by Puck Puck (1947a), once the glycols are embedded in the liquid phase of the bioaerosol droplet, a water/glycol equilibrium is reached, with glycol and water diffusion taking place through the biological membrane, thus inducing membrane alterations and swelling on the viable particles and terminating with inducing microbial osmolysis. Relative humidity and temperature affects the microbicidal effect of glycols, with the most favorable conditions for the biocidal action of PG in its vapor phase given by a temperature below 26° C and relative humidity between 45 % and 70 % (see comprehensive explanation also in Puck (1947b); Puck et al. (1943)).

Puck and coworkers also found that air diluted PG vapor in concentrations of $250-500\,\mathrm{mg/m^3}$ induced an immediate and complete sterilization in an environment in which *Pneumococci*,

Streptococci, *Staphylococci*, *H. Influenzae*, and other microorganisms were suspended. Concentrations of 210 mg/m^3 were sufficient to fully disinfect air in a chamber with suspended *Staphylococcus Albus* after 10 minutes Puck (1947b). Concentrations as low as 50 mg/m^3 were effective against *Pneumococci*. (20). In another study the vaporization of PG was implemented in hospital rooms as preventative mechanism against *Streptococcus Haemolyticus*, under these more diverse environmental conditions regarding temperature and humidity, concentrations over 100 mg/m^3 sustained its bactericidal effect Mather and McClure (1945).

The disinfectant properties of PG and VG that we have described emerged in highly controlled and idealized laboratory and chamber experiments. We discuss in section **??** to what degree these properties could hold under the conditions of real life vaping.

7. Results

7.1. Respiratory droplets emission

From the evidence and data examined in section 3 it is plausible to assume that droplet emission in smoking and vaping (at least MTL style) can be reasonably inferred from outcomes of studies in Table 3 with comparable exhaled tidal volumes (see Table 2), including outcomes of studies mentioned previously that examined breath holds.

The studies we have summarized and listed in Table 3 only involve mouth breathing, but share some common respiratory features with vaping and smoking: oral inspiration with usage of MP's (in vaping), as well as qualitatively similar exhalation velocities and respiratory parameters: inhalation/exhalation times and tidal volumes. However, there are also differences: smoking and vaping do not involve the nose occlusion of these experiments, but involve suction which the subjects of the latter experiments did not experience. While absence of NC's would imply a tidal volume very close to rest values in MTL smoking and vaping, this absence is compensated by the increase due to the need to overcome airflow resistance through suction. The decrease of droplet emission from the mouth/oropharynx hold in MTL topography (absent in normal breathing) was a detected outcome in two of the studies listed in Table 3. We have then the following inferences regarding emission of respiratory droplets

- **MTL vaping and smoking** (and even DTL vaping not involving deep inspiration). The outcomes displayed in Tables 2 and 3 suggest that exhaled droplets in mean tidal volumes $V_T = 700 - 900\,\mathrm{cm}^3$, overwhelmingly in the submicron range (typically peaking at $d_p = 0.3 - 0.8\,\mu\mathrm{m}$), as well as a small rate of droplet emission: roughly $N_p = 6 - 200$ per exhalation (mean $N_p = 79.82$, standard deviation 74.66, computed from the outcomes listed in Table 3 for exhaled volume of 800 cm^3), with droplet number densities well below $n_p = 1\,\mathrm{cm}^{-3}$. However, the wide individual variation reported in these studies should also apply to vaping, including the existence of a small minority of outlier individuals that can be thought of as "super emitters" reaching over $N_p \sim 1000$ per exhalation.

- **DTL vaping**. It involves a spectrum of deeper respiratory intensity than MTL vaping and thus should involve a higher rate of droplet emission. Perhaps the closest analogue in the studies listed in Table 3 to infer droplet emission for intense DTL (2-3 LT exhalation) breathing at fractional residual capacity in Almstrand et al. (2010) that reported emission rates of around 1000/LT. However, this style of vaping is practiced by a small minority of vapers (roughly 10-20 %, see figure 1), while extreme vaping with big clouds (the so called "cloud chasers") is even less frequently practiced in competitions or exhibitions.

Evidently, this type of extreme vaping cannot be sustained for long periods and is not representative even of DTL vapers.

While the inferred droplet numbers in the upper end of high intensity DTL vaping can be comparable with low end numbers for vocalizing, the latter involves modes with larger mean diameters because of distinct droplet generation processes Asadi et al. (2019); Morawska et al. (2009); Johnson et al. (2011).

7.2. Visualization of the respiratory flow

As opposed to other respiratory expirations (breathing, vocalizing, coughing, sneezing), bystanders can actually see the respiratory flow of ECA expirations. This feature has important safety implications that we discuss in section 8.2.1. In section 2.3 we discussed the fluid dynamical property that assures that submicron droplets (ECA and respiratory) actually follow the fluid flow. We provide here a brief discussion of optical properties of aerosols that allow for their visualization (see comprehensive explanation in Ruzer and Harley (2012); Hinds (1999); Kulkarni P and K (2011)).

Visualization and coloring of aerosols follow from the interaction of light with its particulate phase through absorption and scattering (refraction, reflection and difraction), which depends on the particles' number density n_p, chemical nature and the ratio of their diameters to visible light wavelengths: $\alpha = \pi d_p/\lambda$ with $\lambda = 0.4 - 0.7\,\mu$m. This interaction is described in relatively simple terms for ultra-fine particles ($d_p < 0.05\,\mu$m or $\alpha \ll 1$) by Rayleigh's molecular scattering theory and for large particles with $d_p > 100\,\mu$m in terms of geometric optics. Particles with diameters in the intermediate range correspond to Mie scattering theory, which becomes particularly complicated for d_p roughly comparable to λ or $\alpha \approx \pi$, as is the case for ECA and respiratory droplets. Since the latter are liquid droplets, they are in practice non-absorbing so that scattering is the dominant effect.

A simpler approach to aerosol optics follows from the notion of light extinction, the loss of intensity I from absorption and scattering in the direction of an incident parallel non-polarized light beam, with intensity I_0, crossing a distance L within an aerosol. This is described by the extinction coefficient σ_e through the Lambert-Beer (or Bouguer) law

$$I = I_0\, \mathrm{e}^{-\sigma_e L}, \qquad \sigma_e = \frac{\pi}{4} Q_e n \bar{d}^2, \tag{19}$$

where n is the total particle number density, $\bar{d}$ is the mean particle diameter and, for non-absorbing particles, $Q_e \approx Q_{\text{scatt}}$ is the scattering extinction efficiency taken as constant (a valid approximation for a fixed λ and a very small diameter range around $\bar{d}$).

The fact that n in non-biological aerosols (like exhaled ECA) is much larger than in bioarosols that are just "airborne" without ECA (as in "normal" respiratory activities) explains why exhaled ECA is visible while the bioaerosols are not. To illustrate this point quantitatively, consider the light extinction law (19) for an incident beam with wavelength $\lambda = 0.5\,\mu$m crossing an exhaled ECA jet (see figure 3). From the mean diameters obtained in sections 2.2 and 7.1, we have $\bar{d} = \lambda = 0.5\,\mu$m and $\bar{d} = 0.4\,\mu$m for respiratory and ECA droplets (the latter just at exhalation before their rapid evaporation), while (from figure 16.2 of Hinds (1999)) we have $Q_e = 2$, 3.5 respectively for ECA and respiratory droplets, as their respective refractive indices are roughly those of water and VG: $m = 1.33$, 1.5. While L is the same (same fluid jet) and $\bar{d}$ and Q_e have comparable values for both types of droplets, the large difference in n makes a significant effect in light transmission through the beam that indicates the aerosol visibility in its specific direction

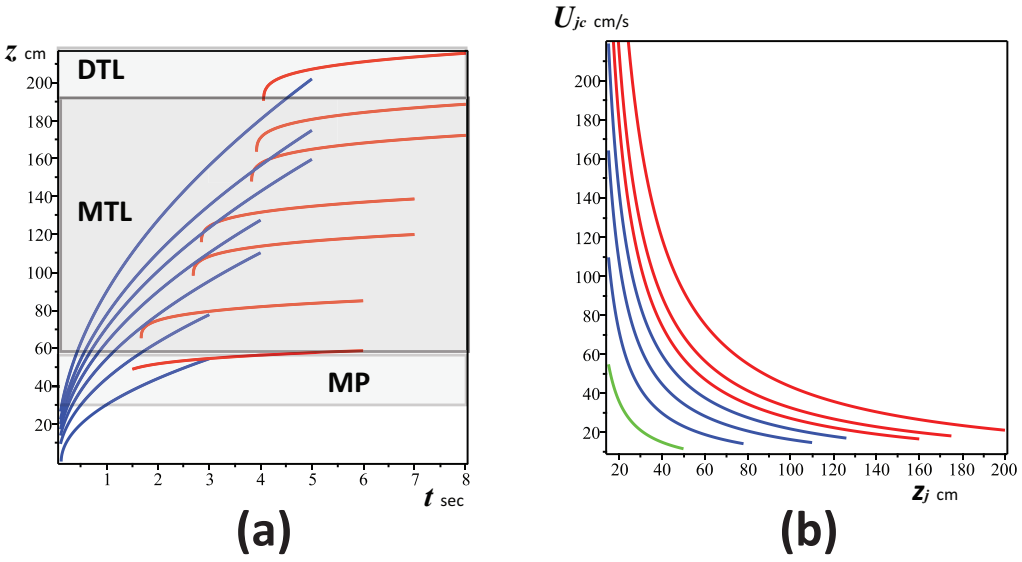

Figure 4: Jet/Puff horizontal displacement and centerline velocity. Panel (a) displays the displacement z_{jc} of the staring jet (blue) and z_{pc} of the puff (red) as functions of time from (equations (7)–(10)), for the three vaping topographies described in section 2.1: DTL (Direct to Lung), MTL (Mouth to Lung) and MP (Mouth Puffing). We assumed as injection (exhalation times) 3, 4 and 5 seconds. The initial velocities from top to bottom are $U_0 = 50, 100, 150, 200, 250, 300, 400$ cm/s. Panel (b) depicts centerline velocities U_c for the starting jet (equation (8)), as functions of the horizontal displacement z_{jc} during the injection times and initial velocities of panel (a) (green for MP, blue for MTL and red for DTL). Notice that once injection stops the jet has reached velocities comparable to those of indoor air currents.

if $I/I_0 < 1$. In numbers: we have $n \sim 10^7\,\text{cm}^{-3}$ and $L = 15\,\text{cm}$ for ECA just at exhalation, leading to impaired light transmission, $I/I_0 = 0.51$, while at 1 meter distance after significant dilution: $\bar{d} \sim 0.1$, $L = 25\,\text{cm}$ and $n \sim 10^5\,\text{cm}^{-3}$, we have almost full light transmission $I/I_0 = 0.99$. For respiratory droplets $n \sim 0.1 - 1\,\text{cm}^{-3}$, leading to practically full light transmission $I/I_0 \approx 1$ irrespective of L (in the appropriate ranges delineated by the exhaled jet).

Extinction through a parallel beam provides a limited description of light scattering in an aerosol, which occurs through each droplet in all directions. The rigorous description through Mie scattering theory is beyond the scope of this paper, but it is evident that droplet numbers play a significant role since total scattered intensity is basically the sum of scattered intensity from each droplet. The light extinction law (19) is valid under the assumption that photons in all directions follow classical paths and their scattering complies with a Poisson distribution (a good approximation for sufficiently diluted aerosols). Under these assumptions the mean free path between scattering events is simply (see chapter 13 of Kulkarni P and K (2011)) $\ell = 1/\sigma_e = 1/(C_e\, n)$, where $C_e \propto \bar{d}^2$ is the extinction cross section per droplet. Evidently, light scattering in the scales of the ECA jet is negligible for bio-aerosols with very low n, as the mean free path ℓ becomes extremely large (much larger than the bio-aerosol scale). For $\bar{d} = 0.5\,\mu\text{m}$, $Q_e = 2$ and $n \sim 0.1 - 1\,\text{cm}^{-3}$ we have $\ell \to 10^8 - 10^9\,\text{cm} = 10^3 - 10^4\,\text{km}$, a huge value that explains the practical lack of scattering events in these bio-aerosols.

7.3. Distance for direct exposure

Direct exposure to respiratory droplets carried by exhaled ECA can be inferred from the horizontal displacement or penetration distance of the jet/puff system whose dynamics follows from equations (7)–(10) with the parameter values in (11)–(12). We display in figure 4 displacement distances and centerline velocities for assorted values of initial exhalation velocities U_0 corresponding to the vaping intensities we have considered.

Notice that the maximal penetration goes beyond that afforded by the momentum trust of the starting jet, with the puff further evolving at lesser speeds. Horizontal penetration varies from 0.5 meters for Mouth Puffing ($U_0 = 0.5$ m/s) through the range between 0.6 and 2.0 meters the MTL regime ($U_0 = 0.3 - 3$ m/s) and beyond 2 meters for the higher intensity DTL regime ($U_0 = 1.5 - 4$ m/s). Centerline velocity drops to about 0.2 m/s at different times and distances when fluid injection stops in all cases.

Given its short time duration and close distance scope of the momentum trusted staring jet, the analytic model (7)–(8) remains a reasonably good approximation to infer the necessary distance to minimize the risk of direct exposure of bystanders to respiratory droplets. As the jet evolves while fluid is injected there is increasing entrainment from the surrounding air at velocity $U_e \propto U_r$, with entrained air reaching about 40 % of the jet mass at the end of injection in the transition towards the puff (around its virtual origin) Ghaem-Maghami (2006); Ghaem-Maghami and Johari (2010). Since there are airflow currents of $\sim$ 10 cm/s (and up to 25 cm/s) even in still air in home environments with natural ventilation Matthews et al. (1989); Berlanga et al. (2017), at this stage the puff formation can be easily destabilized by vortex motion generated through turbulent mixing from the large velocity fluctuations produced by the entrainment Wei and Li (2015); Vuorinen et al. (2020).

Turbulence and thermal buoyancy become important factors when there is human motion or walking Wang and Chow (2011), or in micro-environments with mechanical ventilation (mixed or displaced) He et al. (2011); Gao and Niu (2007); Gao et al. (2008), resulting in a faster disruption and dispersion of the slow moving puff, carrying the submicron ECA and respiratory droplets along the air flow. In general, submicron droplets exhaled at the velocities under consideration can remain buoyant for several hours, with mixing ventilation tending to uniformly spread them, whereas directed ventilation tends to stratify them along different temperature layers. In all cases there is a risk of indirect contagion by exposure to these droplets. The detailed description of droplet dispersion after the puff is disrupted is a complicated process that requires computational techniques that are beyond the scope of this paper (see comprehensive analysis in Vuorinen et al. (2020)).

7.4. Estimation of exposure risks

To evaluate the risk of exposure to respiratory droplets carried by vaping exhalations in indoor environments we have adapted in section 5 the "dose response exponential model" developed by Bounnano, Morawska and Stabile (BMS) Buonanno et al. (2020a) [4] . Specifically, we evaluate equation (17) that defines the risk R (as a fraction < 1) for the value $\mathtt{IR} = 0.96\mathrm{m}^3/\mathrm{h}$ taken from the previous paper of BMS Buonanno et al. (2020b) and justified as a level of physical activity half way between standing and light activity. For the remaining parameters BSM assume the range $\mathtt{AER} = 0.2 - 0.5/h$ for natural ventilation and $\mathtt{AER} = 9.6/h$ for a restaurant scenario with mixed ventilation. BMS compute the deposition rate by dividing typical gravitational settling

[4] We do not assume face mask wearing in this subsection. Effects of face masks are discussed in subsection 7.5.

velocity for supermicron particles (10^{-4} m/s) by the height of emission (1.5 m), leading to $\kappa = 0.24/h$, while for the viral inactivation they take the measured aerosolized SARS-CoV-2 virus mean life of 1.1 hours Van Doremalen et al. (2020) and even longer periods Fears et al. (2020), leading to $\lambda = 0.63/h$. We consider the following home and restaurant indoor scenarios:

- Home scenario. We assume one infectious vaper and three exposed susceptible family members ($N = 3$). Total exposure time $T = 12$ h. Indoor volume 125 m^3 (small 50 m^2 apartment with roof height of 2.5 m). For natural ventilation: $\texttt{AER} = 0.2/\text{h}$ we have $\texttt{IVVR} = 1.07/\text{h}$.
- Restaurant, natural ventilation with open door. Thirty costumers ($N = 30$), total exposure time $T = 3$ h. Air exchange rate $\texttt{AER} = 0.5/\text{h}$, indoor volume 300 m^3 (100 m^2 area with roof height of 3 m), results in $\texttt{IVVR} = 1.37/\text{h}$
- Same restaurant endowed with mechanical ventilation: $\texttt{AER} = 9.6/\text{h}$ (taken from Buonanno et al. (2020b)), results in $\texttt{IVVR} = 10.47/\text{h}$

The infection risk R for home and restaurant scenarios is plotted in figures 5 and 6 as a function of time for breathing, low and high intensity vaping, various percentages of time spent speaking and coughing every 2 minutes, considering natural and mechanical ventilation. As expected from the quanta emission rates displayed in figure 3, the exposure time of different expirations is a crucial factor in computing R. Exposure to vaping expiration (vaper doing 10 puffs per hour) poses an infection risk to bystanders that is very close to that from the control case scenario: exclusive normal rest breathing (for low intensity vaping the infection risk is practically indistinguishable). The infection risk from a person vaping is well below that from the same person speaking and coughing: speaking only for 10 % of the time (6 minutes per hour) already yields a higher infection risk than high intensity vaping, while speaking 30 – 40 % yields up tp 4 times the infection risk, which is roughly the values plotted in figure 7.

A good inference of the risk from intermittent and episodic expiratory activities (vaping, speaking, coughing) relative to the control case scenario of exclusive rest breathing (a continuous expiration) is furnished by the ratio $R_{(\text{A})}/R_{(\text{br})}$, where $A = \text{vp}, \text{sp}, \text{cf}$ (see (16)). Plotting this ratio from (17)–(18) for every expiratory activity yields near constant curves around the values of the quotients $\texttt{ER}_{q(\text{A})}/\texttt{ER}_{q(\text{br})}$ (see numerical values in (16)). This is not surprising since $\texttt{ER}_q$ is the only variable in R that characterizes the infectious person (the other variables characterize the indoor micro-environment and the exposed susceptible persons). Hence, given the same indoor micro-environment and same number of susceptible individuals, we consider risks relative to the control case scenario of rest breathing in terms of the ratio of quanta emission. Using (15) we have

$$\varepsilon = \frac{\texttt{ER}_{q(\text{A})}}{\texttt{ER}_{q(\text{br})}} = 1 + \left(\frac{\mathcal{V}_{d(\text{A})}}{\mathcal{V}_{d(\text{br})}} - 1\right) \approx \frac{R_{(\text{A})}}{R_{(\text{br})}}, \tag{20}$$

where $\mathcal{V}_{d(\text{A})} = V_{T(\text{A})}\, C_{d(\text{A})}$ is the total exhaled droplet volume (in mL) for each expiratory activity "A". Since $N_{(\text{br})} = N_{(\text{tot})}$, then for a heavy breathing activity in intense aerobic exercise ε might grow only because of the much larger tidal volume. However, for a truly intermittent expiration like vaping we have $N_{(\text{vp})}/N_{(\text{br})} \ll 1$ and thus $\varepsilon \approx 1$ holds even if we have $\mathcal{V}_{d(\text{A})}/\mathcal{V}_{d(\text{br})} \gg 1$ (large exhaled amount of droplets as with the large tidal volumes in extremely intense vaping). For the values of tidal volume and droplet volume concentration we have used the numerical values in (16), we have the following relative risks

$$\varepsilon \;=\; 1.25 \times \frac{N_{(\text{vpL})}}{N_{(\text{br})}} \;\text{(low intensity vaping)}, \quad \varepsilon = 5 - 11 \times \frac{N_{(\text{vpH})}}{N_{(\text{br})}} \;\text{(high intensity vaping)},$$

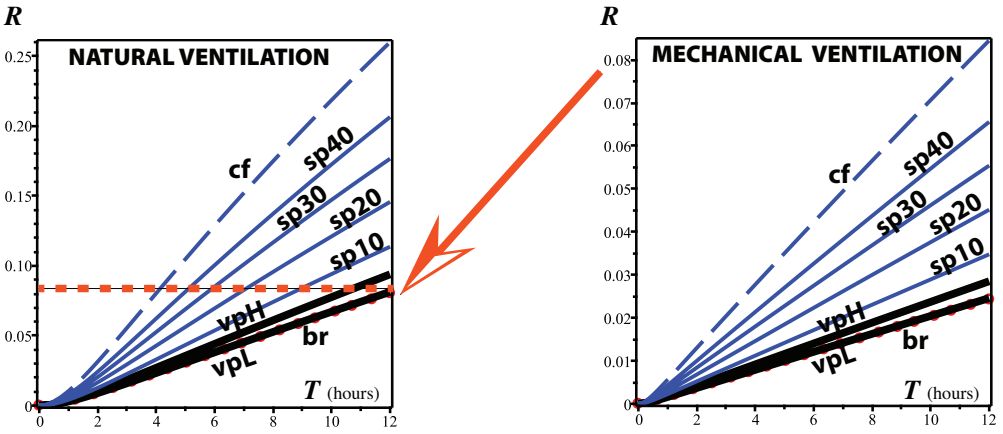

Figure 5: **Infection risk in a home environment.** The curves display R as a function of exposure time T from (17). The abbreviations br, vpL, vpH, sp10, sp20, sp30, sp40 and cf stand for rest breathing, vaping low intensity, vaping high intensity (upper end option), speaking for $10, 20, 30, 40, \%$ of time and coughing. Notice the dramatic reduction of R achieved by mechanical ventilation (air exchange rate of 3/h). Also: the curves for the risks from vaping (all intensities) are practically indistinguishable from that of the case control scenario of rest breathing (red circles).

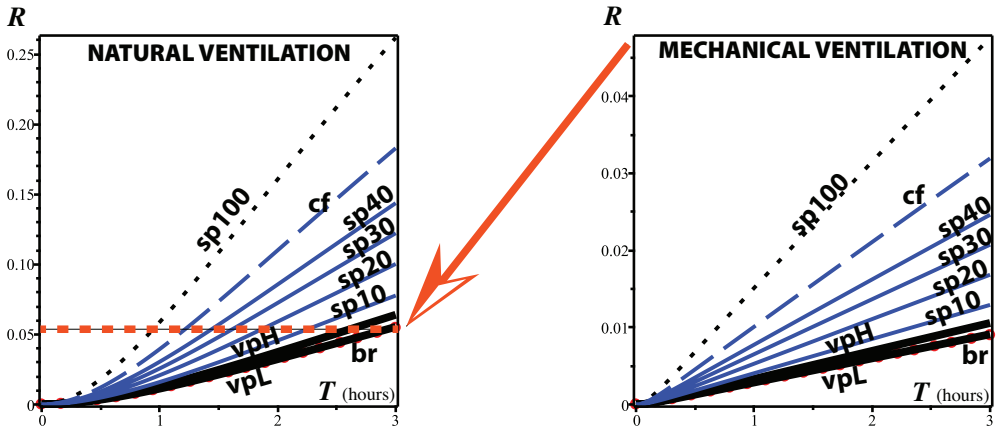

Figure 6: **Infection risk in a restaurant.** The same abbreviations as in figure 5 plus sp100 (speaking 100 % of the time, a possible outcome when spending 3 hours in a restaurant). As in figure 5, mechanical ventilation (air exchange rate 9.6/h) achieves a dramatic reduction of R and the curves for the risks from vaping are practically indistinguishable from the curve of the control case scenario of rest breating (red circles).

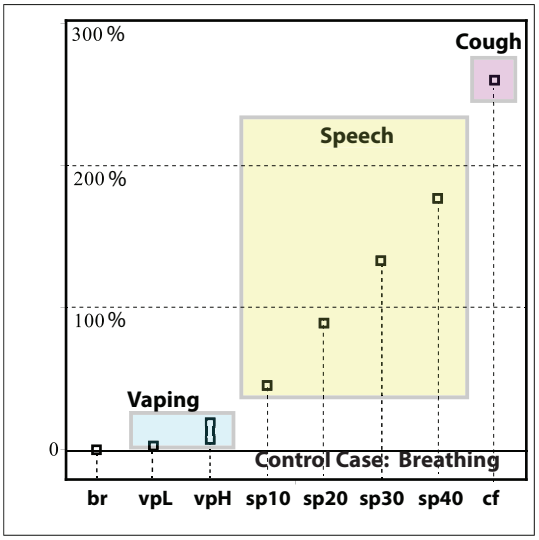

Figure 7: **Added percentage risks of expiratory activities with respect to the control case scenario of rest breathing.** The percentage values with respect to the control case are: low intensity vaping 1.3 % (vpL), high intensity vaping 5.2-17.7 % (vpH), speaking 44% (sp10), 88% (sp20), 132% (sp30), 176% (sp40) for 10%, 20%, 30%, 40% of time, coughing 259% 30 times per hour (cf). These values were obtained from $(\varepsilon - 1) \times 100$ for ε defined for these expiratory activities by (20)–(22).

(21)

$$\varepsilon = 3.6 \times \frac{N_{(\mathrm{sp})}}{N_{(\mathrm{br})}} \text{ (speaking)}, \quad \varepsilon = 28 \times \frac{N_{(\mathrm{cf})}}{N_{(\mathrm{br})}} \text{ (coughing)}, \tag{22}$$

which provides an intuitive indication of the added exposure risks relative to the control case from the different expiratory activities.

We display in figure 7 the numerical values of ε, as an added risk with respect to the control case for various expiratory activities with respect to the continuous presence of risk from rest breathing and under the assumptions we have used. These numbers clearly reflect the effects of the intermittence or duration time of each activity. Under normal vaping conditions (10-15 puffs per hour) the added risk of low intensity vaping respect to the control scenario of exclusive rest breathing is of the order of ~ 1 % (since $\varepsilon - 1 \sim 10^{-2}$). For high intensity vaping it is $\sim 5 - 17$ %, given the ambiguity in the range of $\mathcal{V}_d = V_T C_d$, still it is of the order of $\varepsilon - 1 \sim 5 \times 10^{-2} - 10^{-1}$, also a low added risk since the low value of $N_{(\mathrm{vp})}/N_{(\mathrm{br})}$ compensates for the large exhaled tidal volume. Notice that the added risk respect to the control case grows to ~ 40 % just for talking for 10 % of the time and easily reaches 176 % if talking 40 % of the time. Coughing is also intermittent, possibly even more intermittent than vaping, but its large amount of exhaled droplets (large factor of 28 in (22)) can offset this effect. For speaking ε can be large even if normal speech involves a tidal volume close to rest breathing, but it also involves a much larger amount of time (larger number of breaths in typical conversation).

7.5. Effects of universal face mask wearing

In our risk evaluation in a home and restaurant scenarios we did not assume face mask wearing by emitters and receivers of infective quanta. However, while other respiratory activities can

proceed when face mask are worn, vaping necessarily requires their removal at least for the brief time lapse of intermittent puffs. This fact has little real life relevance in our risk evaluation for the home scenario because face mask are rarely worn at home (even under confinement). Assuming that containment measures permit that bars and restaurants remain open, our risk evaluation also remains roughly valid for such venues (if vaping is allowed), as eating and drinking also require face mask removal, which in a convivial atmosphere (with conversations accompany eating and drinking) should involve quanta emissions by mask-free patrons whose duration is likely to exceed the strict time needed to eat and drink. However, it is still necessary to examine exposure risks in hypothetical indoor scenarios in which universal face mask wearing is strictly enforced. In particular, we need to emphasize the effects on those face masks that are usually worn at a community level: surgical masks and/or those made of cotton and other fabrics.

Face masks, in their multiple designs and fiber characteristics (see review in Tcharkhtchi et al. (2020)), filter aerosol particles through various physical processes: gravitational sedimentation, inertial impaction, interception, diffusion and electrostatics, each of which govern and/or becomes dominant in specific ranges of particle sizes, airflow, leaks and environmental factors according to aerosol filtering theory Hinds (1999). The key issue we need to assess is how much cotton and surgical masks protect (in terms of filtering efficiency) their wearers from *inward* emission when they are exposed to *outward* quanta emissions by potentially infectious individuals not wearing face masks (as vapers when vaping). It is especially useful to compare this protection with respect to the one they would get when exposed to emitters who are also masked (*i.e. reciprocal masking*).

Filtering efficiency is high in outward emission for N95 respirators (over 90 %) and slightly less so (74 %) in surgical masks in human emitters breathing, speaking and coughing Asadi et al. (2020), with decreasing diameters of filtered droplets, though in these experiments droplet counts excluded ultra-fine droplets below 300 nm and leaks were not evaluated. Similar results were obtained in laboratory conditions with a non-biological aerosol, though leaking decreased efficiency in surgical and cotton masks between one half and two thirds Drewnick et al. (2021).

Evidently, face masks also protect their wearers from inward emissions, as revealed by the following two laboratory experiments:

- In Sickbert-Bennett et al. (2020) two human subjects in different body postures, wearing well fit N95 respirators and surgical masks (tied with stripes or ear loops), were exposed to a non-biological polydisperse aerosol ($d_p = 0.02 - 3.00\,\mu$m) released in a chamber at concentrations between 2000-5000 cm^{-3}. Fitted filtration efficiency was above 95 % in all N95 respirators, 71.5 % for the surgical mask tied with stripes and 38.1 % for the one fit with ear lobes. Efficiency decreased for the latter to 21.2 % when the subjects turned their head left or right, showing the effects of leaks.

- In Ueki et al. (2020) a bio-aerosol generated by a nebulizer emitted at flow velocity of 2 m/s, simulating a mild cough airflow, was used to examine virus penetration (in terms of virus titer) between two mannequins separated at distances of 50 and 100 cm, in experiments wearing loose and fit N95 respirators, surgical and cotton masks. The filtering efficiency was measured in terms of the detected percentage of virus titer in the receiving mannequin with respect to the titer in the emitting one. For 10^5 PFU (plaque forming units) when the receiver was wearing different face masks and the emitter was unmasked filtering efficiency was: 17 %, 47 %, 57 % and 79 % for the cotton mask, surgical mask, loose and fit N95 respirators respectively. When both mannequins wore a surgical mask the filtering efficiency significantly rose to 60 %, 71 %, 69 % and 92 %. Efficiency was

about 10 % lower for 10^8 PFU. Virus titers decreased to 45 % and 31 % when mannequins (both unmasked) were placed at distances of 50 cm and 100 cm with respect to their values at 25 cm separation.

Both laboratory experiments describe, in spite of their idealization, the relatively low protection afforded by cotton and surgical masks to bystanders exposed to either unmasked emitters at close range and/or high droplet concentrations, flow and virus titer, which are precisely the conditions characteristic of direct exposure that would likely affect bystanders (wearing such masks) placed at the source (close to the mouth) of the jet exhaled by an infectious vaper or by someone infectious breathing, talking or coughing without wearing a mask.

However, as opposed to masked bystanders exposed to mask-less emissions from other respiratory activities, bystanders close to a vaper can avoid instinctively the spatial zone of direct exposure that is clearly delineated by the visible emission jet exhaled by a vaper. Bystanders wearing cotton or surgical masks located outside the exhaled jet would be subjected to indirect exposure to a very low concentration of submicron droplet nuclei (the so-called "aerosols") dispersing through air currents at ambient velocities that depend on the ventilation regime (roughly below 10-20 cm/s with natural ventilation Matthews et al. (1989); Berlanga et al. (2017)). These are evidently very different conditions from those of the experiments described above, and thus wearing these masks would offer these bystanders a much higher level of protection.

In particular, a much decreased airflow in indirect exposure implies a much decreased face velocity U_f, the air velocity at the mask surface obtained by dividing the air flow (LT/min) over the mask surface area. Intuitively, under these conditions the masks capture more particles (droplet nuclei) because the permanence time of the latter favors the capture mechanisms that are dominant for this particle size range: diffusion and interception. The dependence of the percentage of filtration efficiency E on U_f when diffusion and interception are dominant is given by $E \propto [1 - \exp(-U_f^{-4/9})] \times 100$ (see equations 9.19 and 9.35 of Hinds (1999)), so that $E \approx 100\,\%$ as U_f decreases to conditions of indirect exposure. The same arguments apply to indirect exposure to drifting droplet nuclei from other respiratory activities that are sufficiently small to remain buoyant for long times.

As a consequence, universal wearing of cotton and surgical face masks practically offers complete protection against indirect exposure to small nuclei spread once respiratory droplets have evaporated. Evidently, it would be extremely complicated to adapt the relative risk model we have presented to these conditions, since we would have to re-calculate in terms of the filtering efficiency of the face masks the quanta emission assigned to the control state of breathing emitters, of the comparative emitters talking and coughing, as well as the exposed receivers. However, incorporating this complexity might not be worthwhile given the fact that SARS-CoV-2 transmission via indirect exposure is still uncertain and controversial NAS (2020); Jayaweera et al. (2020); Shiu et al. (2019).

7.6. Disinfectant properties under realistic vaping conditions

It is difficult to relate the highly controlled and idealized experiments described in section 6 to the erratic and highly variable conditions in vaping. First, as we argued in section 3.3, the desiccating effect of PG and VG is not likely to be effective on the submicron respiratory droplets accompanying exhaled ECA, as the latter are, most likely, desiccated nuclei of evaporated droplets. Second, in these experiments pure PG (as aerosol or as vapor) was supplied continuously and spread evenly under carefully controlled conditions, whereas particulate and gas phase concentrations of ECA rapidly vary with time and position. The gas phase of ECA

is a mixture of PG and other compounds (VG, nicotine, with residual concentrations of mostly aldehydes) and is supplied into the surrounding air (when inhaled or exhaled) intermittently during puffs and spreads rapidly and unevenly. Third, bactericidal effects in these experiments were registered with PG concentrations of: $50 - 500\,\mathrm{mg/m^3}$ which are 2-3 orders of magnitude higher than maximal gaseous PG concentrations of exhaled ECA registered in experiments involving several users vaping in relatively small chambers during hours: $0.3 - 0.4\,\mathrm{mg/m^3}$ Czogala et al. (2014); Liu et al. (2017).

However, the disinfection might be more plausible for inhaled ECA. Since about 92 % of inhaled PG is retained St. Helen et al. (2016), PG concentrations inside the respiratory tracts approach the lower end of concentrations in the experiments and could interact with droplets still in aqueous form. Still, the disinfectant effect is unlikely to occur, as the transit and absorption time of ECA in the respiratory system is too short (around 5-6 seconds) and this effect is much less efficient in the prevailing relative humidity close to 100 %.

As we have argued throughout this article, exhaled ECA (as an expiratory activity) should spread respiratory droplets in the environment. However, it is very unlikely that its chemical medium could inhibit COVID-19 contagion by disabling or destroying the SARS-CoV-2 virus. Conversely, it is equally unlikely that this chemical medium could (somehow) enhance the probability of contagion in comparison with "normal" airborne transmission. Nevertheless, the chemical interaction between the SARS-CoV-2 virus and PG and/or other glycols and compounds of ECA needs to be probed and tested in well designed experiments, even outside the context of vaping.

8. Limitations, final discussion and conclusion

We have presented in this paper a comprehensive analysis and theoretical modeling of the plausibility, scope and risk for pathogen (including SARS-CoV-2 virus) contagion through direct and indirect exposure to respiratory droplets that would be carried by ECA (e-cigarette aerosol) exhaled by vapers. An extended summary that outlines the methodological structure and obtained results of the article is provided in the Introduction.

8.1. Limitations

8.1.1. Lack of empiric data.

It is important to openly recognize the main limitation of this study: the lack of experimental and observational data on respiratory droplets carried by exhaled ECA. It is quite plausible that emission of these droplets should occur, as exhaled ECA is an expiratory activity, but without empiric data any quantitative assessment of its nature and scope must necessarily be inferred or estimated indirectly, either through theoretical speculation from the physical and chemical properties of ECA, or through extrapolation from available data on other expiratory activities that can serve as reasonable proxies for vaping. The need to provide the best possible and self consistent inference on this missing data explains and justifies the length of the present study: data availability would render several sections (for example sections 3.1, 3.2 and 3.3) redundant or drastically shortened and kept only for comparative reference.

8.1.2. Oversimplification of vaping styles.

The classification of puffing topographies in two separate mutually exclusive categories (MTL and DTL) that we presented in section 2.1 roughly conveys the two main vaping styles, but e-

cigarettes are a rapidly changing technology and thus this simplified approach cannot capture the full range and scope of individual vaping habits.

8.1.3. Oversimplification of infective parameters and individual variability.

We remark that the ranges of numerical values we have obtained of emitted droplets possibly emitted by vaping are rough average estimates gathered from outcomes reported in breathing studies (listed in Table 3) involving a wide variety of subjects, including both healthy and individuals affected by respiratory conditions (not by SARS-CoV-2). We have not considered the small minority of outlier individuals who are super spreaders emitting significantly larger numbers of droplets Asadi et al. (2019). We have also considered simply droplet emission, disregarding (up to section 5) the specification of a specific pathogen. Evidently, this oversimplification disregards important known facts, for example: droplet characteristics vary among pathogens and between healthy and infected subjects.

It is worth mentioning that the data on infective SARS-CoV-2 parameters gathered by BMS that we use in section 5 to adapt their risk modeling is also subjected to uncertainties that they specifically recognize. In fact, numerous aspects associated with the spreading and infection details of the SARS-CoV-2 virus remain uncertain and subject to large (often unexplained) individual and environmental variability (a good summary of these uncertainties is found in Klompas et al. (2020); Morawska and Milton (2020); Morawska and Cao (2020); NAS (2020)). However, in order to be able to model a possible (previously unexplored) route of droplet transmission and possible infection, it is necessary and unavoidable to simplify this complexity and lack of data to obtain plausible order of magnitude estimates that can be verified once empiric evidence is available.

8.1.4. Oversimplification of droplet dynamics.

While the simple dynamical modelling of exhaled ECA as a starting jet followed by an unstable puff (section 4) is sufficient to estimate direct exposure distances, we recognize its limitations: it is strictly valid for a jet/puff system emitted by a static vaper in typical indoor conditions. Evidently, to estimate the fluid flows that determine this exposure (and indirect exposure by dispersing droplets) in less idealized conditions requires a more realistic description using computational methods of fluid mechanics to incorporate effects of turbulence and thermal bouyancy, as well as air currents from ventilation or motion. Rather, we examined global volume exposure through a risk model not involving fluid dynamics. It is important to mention that this simplification of the dynamics is harder to justify for expiratory activities like coughing or sneezing, as the latter involve larger ejection velocities and a much wider spectrum of droplet diameters that includes significant number of large supermicron droplets (significant numbers of diameters $1-10\,\mu$m and even $>100\,\mu$m) whose effect on the dynamics of the carrier fluid cannot be neglected (these are strictly speaking multiphasic flows Yeoh and Tu (2019); Scharfman et al. (2016); Bourouiba et al. (2014)).

8.1.5. Oversimplification of the risk model.

The simplified BMS risk model that we presented in section 5 fulfills our aim of providing a rough estimation of relative risks from volume exposure to intermittent vaping expirations with respect to the control case of continuous rest breathing. However, we do recognize its limitations: the risks are evaluated for a single vaper in highly idealized micro-environments, assuming constant infection parameters and inhalation rates (which BMS also assume), ignoring as well probability distributions of the quanta emission rates that convey individual variation on

infection susceptibility and other parameters (which the model of BMS does incorporate). A more elaborate and complete approach should include a more robust methodology to quantify exposure risks to intermittent and sporadic sources, as for example in Nazaroff (2004); Ai et al. (2019). This task is left for a future analysis.

8.2. Safety considerations

8.2.1. Respiratory flow visualization.

Is quite plausible that exhaled ECA (as a respiratory activity) can spread pathogens (including SARS-CoV-2) hosted in respiratory droplets. However, as opposed to other respiratory activities (speaking, singing, coughing, sneezing), the involved respiratory flow is visible because the carried submicron droplets (ECA and respiratory) act effectively as visual tracers of the carrier fluid (see sections 2.3 and 7.2). Besides the evident psychological dimension of this flow visualization, there are safety implications: vapers and those surrounding them have a clear, instinctive and immediate delineation of the flow's horizontal distance reach and spreading direction along the exhaled jet. From the outcomes of our hydrodynamical analysis (section 7.3), we can recommend as a basic safety measure to avoid direct exposure (irrespective of face mask wearing) by keeping a 2 meter distance away from the vaper (when vaping) in the direction of the visible jet. In other directions the exposure is indirect, but nevertheless it is prudent to maintain 2 meters of separation in all directions from anyone vaping when not wearing a face mask. Notice that these recommended safety measures coincide with the standard social separation recommendations adopted worldwide Hsiang et al. (2020).

8.2.2. Airborne "aerosols" vs "droplets".

Their overwhelmingly submicron range makes respiratory droplets potentially carried by exhaled ECA well within the range of droplet sizes that the WHO (and most medical literature) conventionally denotes by the term "aerosols" (*i.e.* droplets with $d_p < 5\,\mu$m, as opposed to the term "droplets" applied to $d_p > 5\,\mu$m). As we mentioned in the introduction, there is indisputable evidence that indirect exposure to "aerosols" has contributed to SARS-CoV-2 contagion, specially in hospital wards Liu et al. (2020); Li et al. (2020); Lu et al. (2020) and clusters in housing and public transport Cai et al. (2020); Shen et al. (2020). It has been suggested that contagion from "aerosols" play an important role, with authors calling for mitigating measures to better address this issue Klompas et al. (2020); Morawska and Milton (2020); Morawska and Cao (2020), arguing to support their case that besides the contagion cases cited before there is experimental evidence that airborne SARS-CoV-2 virus in artificially generated aerosols has remained viable and stable for periods of typically 3 hours Van Doremalen et al. (2020); Fears et al. (2020) (and up to 16 hours in Fears et al. (2020)). They also point out findings of SARS-CoV-2 viral RNA in ventilation systems of hospital rooms Zhou et al. (2020); Chia et al. (2020). However, the scope and importance of this indirect contagion remains controversial (see reviews in Jayaweera et al. (2020); Shiu et al. (2019)), as there are counter arguments to the claims supporting its prominence: in experiments detecting hours long airborne viability of the SARS-CoV-2 virus Van Doremalen et al. (2020); Fears et al. (2020) the carrying aerosols were generated and examined under extremely idealized laboratory conditions that might be unrepresentative of submicron droplet (*i.e.* "aerosols") generation in the respiratory system and of realistic evolution of bioaerosols in indoor and outdoor environments. Also, detected RNA of SARS-CoV-2 does not necessarily indicate the presence of a viable infectious virus Bullard et al. (2020).

8.2.3. Face masks.

In computing exposure risks in section 7.4 we did not consider face mask wearing, an assumption, which as mentioned in section 7.5, is justified because this protective gear is usually not worn in a home scenario. Even in a restaurant or bar scenario, patrons are likely to remain mask-less for extended periods because masks must be removed for eating and drinking (as with vaping). As we showed in section 7.5, face masks of common usage (surgical and cotton) afford limited protection to bystanders wearing them who might be subjected to direct exposure to respiratory droplets from mask-free emitters, as it would happen if directly exposed to droplet emissions by an infectious vaper. However, bystanders can easily (and instinctively) avoid this risky exposure by placing themselves outside the zone of direct exposure delineated by the visible exhaled jet, something difficult (or impossible) to do with other respiratory activities whose zone of direct exposure is invisible. Once outside the direct exposure zone, bystanders wearing common usage face masks would be effectively protected from indirect exposure to dispersing submicron droplet nuclei remaining buoyant for extended periods.

8.2.4. Lockdown vs opening.

Risk assessments are essential to provide evidence based support for preventive and mitigating policies that have been proposed and enacted worldwide (see review Hsiang et al. (2020)). These assessments are sensitive to the wide variety of rapidly changing pandemic conditions and scenarios. High levels of severity characterized by frequent contagion rates can be addressed by lockdowns contemplating different levels and stages of home confinement. Under these conditions the risk assessment for the home scenario that we presented is particularly relevant, as a large number of vapers and smokers become home bound for a range of large periods. Our risk assessment provides valuable information for safety policies in this scenario: low intensity vaping only produces a minuscule ($\sim 1\,\%$) extra contagion risk with respect to the control case scenario of continuous breathing. Safety interventions should consider that abstention from vaping would not produce a noticeable safety improvement, but could generate an undesired level of stress and anxiety under long term confinement. High intensity vaping produces a higher increase of relative risk, but still well below speaking and coughing. Notice that face masks are seldom worn in home bound scenarios of family clusters.

While vaping bans inside homes would be an extremely intrusive intervention, many jurisdictions might prohibit vaping in closed publicly shared indoor spaces (malls, bus and train terminals, airports, restaurants, etc), but there are shared spaces, such as covered terraces in bars and restaurants, where vaping is more likely allowed and might be open to the public under less severe pandemic conditions that allow a measure of social activity. Our risk analysis is also useful for medical personnel, pharmacists, supermarket workers, couriers, policemen, police women and other providers of essential services who might dwell in indoor and outdoor spaces in which vaping is allowed.

8.2.5. Final conclusion.

The standard recommendation of keeping a 2 meters social separation distance is sufficient to address the risk of direct contagion through exhaled ECA potentially carrying the SARS-CoV-2 virus. As far as protection from exposure to respiratory droplets in general, those sharing indoor spaces with vapers do not require extra safety interventions besides those already recommended for the general population: wearing face masks besides the separation distance to avoid direct exposure. Setting aside harms from environmental tobacco smoke unrelated to COVID-19, these recommendations also apply to sharing an indoor space with a smoker.

Competing interests

RAS has no competing interests to declare.

EG is currently employed by Myriad Pharmaceuticals, an independent company that manufactures e-liquids and vaping devices in New Zealand. She also provides consultancy work on research and development, regulatory affairs support, and formulation to several independent vaping companies in the Pacific Region. In the past she has worked for several pharmaceutical companies, including GlaxoSmithKline and Genomma Lab. She is also a member of the standards committee of the VTANZ and UKVIA.

RP is full time employee of the University of Catania, Italy. In relation to his work in the area of tobacco control and respiratory diseases, RP has received lecture fees and research funding from Pfizer, GlaxoSmithKline, CV Therapeutics, NeuroSearch A/S, Sandoz, MSD, Boehringer Ingelheim, Novartis, Duska Therapeutics, and Forest Laboratories. He has also served as a consultant for Pfizer, Global Health Alliance for treatment of tobacco dependence, CV Therapeutics, NeuroSearch A/S, Boehringer Ingelheim, Novartis, Duska Therapeutics, Alfa-Wassermann, Forest Laboratories, ECITA (Electronic Cigarette Industry Trade Association, in the UK), Arbi Group Srl., and Health Diplomats. RP is the Founder of the Center of Excellence for the acceleration of Harm Reduction at the University of Catania (CoEHAR), which has received a grant from Foundation for a Smoke Free World to develop and carry out 8 research projects. RP is also currently involved in the following pro bono activities: scientific advisor for LIAF, Lega Italiana Anti Fumo (Italian acronym for Italian Anti Smoking League) and Chair of the European Technical Committee for standardization on Requirements and test methods for emissions of electronic cigarettes (CEN/TC 437; WG4)

References

, September 1980. Air sanitizers. dis/tss-11 / efficacy data and labelling requirements. [online]. Available at https://archive.epa.gov/pesticides/oppad001/web/html/dis-11.html, cited: 10 13, 2020.

, 2000a. Pubchem compound summary for cid 1030, propylene glycol. Available at https://pubchem.ncbi.nlm.nih.gov/compound/Propylene-glycol, pubChem Database. Retrieved October 28, 2020.

, 2000b. Pubchem compound summary for cid 763, glycerol. Available at https://pubchem.ncbi.nlm.nih.gov/compound/Glycerol, pubChem Database. Retrieved October 28, 2020.

, 2017. Propylene glycol used as an excipient report published in support of the 'questions and answers on propylene glycol used as an excipient in medicinal products for human use' (ema/chmp/704195/2013). Available at https://www.ema.europa.eu/en/documents.

, 2020. Airborne Transmission of SARS-CoV-2: Proceedings of a Workshop in Brief. National Academies of Sciences, Engineering, and Medicine, The National Academies Press, Washington, DC.

, 2020. Ecig intelligence: Databases - key global analysis of the vapour sector. https://ecigintelligence.com/content_types/database/, retrieved October 28, 2020.

Abani, N., Reitz, R. D., 2007. Unsteady turbulent round jets and vortex motion. Physics of Fluids 19 (12), 125102.

Abraham, J., 1996. Entrapment characteristics of transient gas jets. Numerical Heat Transfer, Part A Applications 30 (4), 347–364.

Ai, Z., Hashimoto, K., Melikov, A. K., 2019. Airborne transmission between room occupants during short-term events: Measurement and evaluation. Indoor air 29 (4), 563–576.

Ai, Z., Mak, C. M., Gao, N., Niu, J., 2020. Tracer gas is a suitable surrogate of exhaled droplet nuclei for studying airborne transmission in the built environment. In: Building Simulation. Springer, pp. 1–8.

Almstrand, A.-C., Bake, B., Ljungström, E., Larsson, P., Bredberg, A., Mirgorodskaya, E., Olin, A.-C., 2010. Effect of airway opening on production of exhaled particles. Journal of applied physiology 108 (3), 584–588.

Asadi, S., Cappa, C. D., Barreda, S., Wexler, A. S., Bouvier, N. M., Ristenpart, W. D., 2020. Efficacy of masks and face coverings in controlling outward aerosol particle emission from expiratory activities. Scientific reports 10 (1), 1–13.

Asadi, S., Wexler, A. S., Cappa, C. D., Barreda, S., Bouvier, N. M., Ristenpart, W. D., 2019. Aerosol emission and superemission during human speech increase with voice loudness. Scientific reports 9 (1), 1–10.

Asgharian, B., Price, O. T., Rostami, A. A., Pithawalla, Y. B., 2018. Deposition of inhaled electronic cigarette aerosol in the human oral cavity. Journal of Aerosol Science 116, 34–47.

Askanazi, J., Silverberg, P., Foster, R., Hyman, A., Milic-Emili, J., Kinney, J., 1980. Effects of respiratory apparatus on breathing pattern. Journal of Applied Physiology 48 (4), 577–580.

Bailey, E. F., Hoit, J. D., 2002. Speaking and breathing in high respiratory drive. Journal of Speech, Language, and Hearing Research.

Bake, B., Larsson, P., Ljungkvist, G., Ljungström, E., Olin, A., 2019. Exhaled particles and small airways. Respiratory research 20 (1), 8.

Berlanga, F., Olmedo, I., Ruiz de Adana, M., 2017. Experimental analysis of the air velocity and contaminant dispersion of human exhalation flows. Indoor Air 27 (4), 803–815.

Bernstein, D. M., 2004. A review of the influence of particle size, puff volume, and inhalation pattern on the deposition of cigarette smoke particles in the respiratory tract. Inhalation toxicology 16 (10), 675–689.

Bourouiba, L., Dehandschoewercker, E., Bush, J. W., 2014. Violent expiratory events: on coughing and sneezing. Journal of Fluid Mechanics 745, 537–563.

Brief, S., 2020. Sars-cov-2 and potential airborne transmission. cdc. org.

Bullard, J., Dust, K., Funk, D., Strong, J. E., Alexander, D., Garnett, L., Boodman, C., Bello, A., Hedley, A., Schiffman, Z., et al., 2020. Predicting infectious sars-cov-2 from diagnostic samples. Clinical Infectious Diseases.

Buonanno, G., Morawska, L., Stabile, L., 2020a. Quantitative assessment of the risk of airborne transmission of sars-cov-2 infection: prospective and retrospective applications. medRxiv.

Buonanno, G., Stabile, L., Morawska, L., 2020b. Estimation of airborne viral emission: quanta emission rate of sars-cov-2 for infection risk assessment. Environment International, 105794.

Cahours, X., Prasad, K., 2018. A review of electronic cigarette use behaviour studies. Beiträge zur Tabakforschung International/Contributions to Tobacco Research 28 (2), 81–92.

Cai, J., Sun, W., Huang, J., Gamber, M., Wu, J., He, G., 2020. Indirect virus transmission in cluster of covid-19 cases, wenzhou, china, 2020. "Emerging Infectious Diseases, 26(6), 1343-1345. https://dx.doi.org/10.3201/eid2606.200412".

Cameron, P. U., Pagnon, J. C., van Baare, J., Reece, J. C., Vardaxis, N. J., Crowe, S. M., 2000. Efficacy and kinetics of glycerol inactivation of hiv-1 in split skin grafts. Journal of medical virology 60 (2), 182–188.

Chao, C. Y. H., Wan, M. P., Morawska, L., Johnson, G. R., Ristovski, Z., Hargreaves, M., Mengersen, K., Corbett, S., Li, Y., Xie, X., et al., 2009. Characterization of expiration air jets and droplet size distributions immediately at the mouth opening. Journal of Aerosol Science 40 (2), 122–133.

Charles, F., Krautter, G. R., Mariner, D. C., 2009. Post-puff respiration measures on smokers of different tar yield cigarettes. Inhalation toxicology 21 (8), 712–718.

Chen, C., Zhao, B., 2010. Some questions on dispersion of human exhaled droplets in ventilation room: answers from numerical investigation. Indoor Air 20 (2), 95–111.

Chia, P. Y., Coleman, K. K., Tan, Y. K., Ong, S. W. X., Gum, M., Lau, S. K., Lim, X. F., Lim, A. S., Sutjipto, S., Lee, P. H., et al., 2020. Detection of air and surface contamination by sars-cov-2 in hospital rooms of infected patients. Nature communications 11 (1), 1–7.

Czogala, J., Goniewicz, M. L., Fidelus, B., Zielinska-Danch, W., Travers, M. J., Sobczak, A., 2014. Secondhand exposure to vapors from electronic cigarettes. nicotine & tobacco research 16 (6), 655–662.

Dautzenberg, B., Bricard, D., 2015. Real-time characterization of e-cigarettes use: the 1 million puffs study. J. Addict. Res. Ther 6 (229.10), 4172.

Daynard, R., 2018. Public health consequences of e-cigarettes: a consensus study report of the national academies of sciences, engineering, and medicine.

De Spiegeleer, B., Wattyn, E., Slegers, G., Van der Meeren, P., Vlaminck, K., Van Vooren, L., 2006. The importance of the cosolvent propylene glycol on the antimicrobial preservative efficacy of a pharmaceutical formulation by doe-ruggedness testing. Pharmaceutical development and technology 11 (3), 275–284.

Douglas, N., White, D., Weil, J., Zwillich, C., 1983. Effect of breathing route on ventilation and ventilatory drive. Respiration physiology 51 (2), 209–218.

Drewnick, F., Pikmann, J., Fachinger, F., Moormann, L., Sprang, F., Borrmann, S., 2021. Aerosol filtration efficiency of household materials for homemade face masks: Influence of material properties, particle size, particle electrical charge, face velocity, and leaks. Aerosol Science and Technology 55 (1), 63–79.

Elghobashi, S., 1994. On predicting particle-laden turbulent flows. Applied scientific research 52 (4), 309–329.

Fabian, P., Brain, J., Houseman, E. A., Gern, J., Milton, D. K., 2011. Origin of exhaled breath particles from healthy and human rhinovirus-infected subjects. Journal of aerosol medicine and pulmonary drug delivery 24 (3), 137–147.

Farsalinos, K., Poulas, K., Voudris, V., 2018. Changes in puffing topography and nicotine consumption depending on the power setting of electronic cigarettes. Nicotine and Tobacco Research 20 (8), 993–997.

Farsalinos, K. E., Polosa, R., 2014. Safety evaluation and risk assessment of electronic cigarettes as tobacco cigarette substitutes: a systematic review. Therapeutic advances in drug safety 5 (2), 67–86.

Fears, A. C., Klimstra, W. B., Duprex, P., Hartman, A., Weaver, S. C., Plante, K., Mirchandani, D., Plante, J., Aguilar, P. V., Fernandez, D., et al., 2020. Comparative dynamic aerosol efficiencies of three emergent coronaviruses and the unusual persistence of sars-cov-2 in aerosol suspensions. medRxiv.

Floyd, E. L., Queimado, L., Wang, J., Regens, J. L., Johnson, D. L., 2018. Electronic cigarette power affects count concentration and particle size distribution of vaping aerosol. PloS one 13 (12), e0210147.

Fuoco, F. C., Buonanno, G., Stabile, L., Vigo, P., 2014. Influential parameters on particle concentration and size distribution in the mainstream of e-cigarettes. Environmental pollution 184, 523–529.

Gao, N., Niu, J., 2007. Modeling particle dispersion and deposition in indoor environments. Atmospheric environment 41 (18), 3862–3876.

Gao, N., Niu, J., Morawska, L., 2008. Distribution of respiratory droplets in enclosed environments under different air distribution methods. In: Building simulation. Vol. 1. Springer, pp. 326–335.

Ghaem-Maghami, E., 2006. The passive scalar concentration and velocity fields of isolated turbulent puffs.

Ghaem-Maghami, E., Johari, H., 2010. Velocity field of isolated turbulent puffs. Physics of Fluids 22 (11), 115105.

Gilbert, R., Auchincloss Jr, J., Brodsky, J., Boden, W. a., 1972. Changes in tidal volume, frequency, and ventilation induced by their measurement. Journal of Applied Physiology 33 (2), 252–254.

Gralton, J., Tovey, E., McLaws, M.-L., Rawlinson, W. D., 2011. The role of particle size in aerosolised pathogen transmission: a review. Journal of Infection 62 (1), 1–13.

Grégory, D., Parmentier, E. A., Irene, T., Ruth, S., 2020. Tracing the composition of single e-cigarette aerosol droplets in situ by laser-trapping and raman scattering. Scientific Reports (Nature Publisher Group) 10 (1).

Gupta, J., Lin, C.-H., Chen, Q., 2009. Flow dynamics and characterization of a cough. Indoor air 19 (6), 517–525.

Gupta, J. K., Lin, C.-H., Chen, Q., 2010. Characterizing exhaled airflow from breathing and talking. Indoor air 20 (1), 31–39.

Haslbeck, K., Schwarz, K., Hohlfeld, J. M., Seume, J. R., Koch, W., 2010. Submicron droplet formation in the human lung. Journal of Aerosol Science 41 (5), 429–438.

He, Q., Niu, J., Gao, N., Zhu, T., Wu, J., 2011. Cfd study of exhaled droplet transmission between occupants under different ventilation strategies in a typical office room. Building and Environment 46 (2), 397–408.

Herning, R. I., Hunt, J. S., Jones, R. T., 1983. The importance of inhalation volume when measuring smoking behavior. Behavior Research Methods & Instrumentation 15 (6), 561–568.

Higenbottam, T., Feyeraband, C., Clark, T., 1980. Cigarette smoke inhalation and the acute airway response. Thorax 35 (4), 246–254.

Hinds, W. C., 1999. Aerosol technology: properties, behavior, and measurement of airborne particles. John Wiley & Sons.

Hirsch, J., Bishop, B., 1982. Human breathing patterns on mouthpiece or face mask during air, co2, or low o2. Journal of Applied Physiology 53 (5), 1281–1290.

Holmgren, H., Gerth, E., Ljungström, E., Larsson, P., Almstrand, A.-C., Bake, B., Olin, A.-C., 2013. Effects of breath holding at low and high lung volumes on amount of exhaled particles. Respiratory physiology & neurobiology 185 (2), 228–234.

Holmgren, H., Ljungström, E., Almstrand, A.-C., Bake, B., Olin, A.-C., 2010. Size distribution of exhaled particles in the range from 0.01 to 2.0 μm. Journal of Aerosol Science 41 (5), 439–446.

Hoshiko, M. S., 1965. Lung volume for initiation of phonation. Journal of applied physiology 20 (3), 480–482.

Hsiang, S., Allen, D., Annan-Phan, S., Bell, K., Bolliger, I., Chong, T., Druckenmiller, H., Huang, L. Y., Hultgren, A., Krasovich, E., et al., 2020. The effect of large-scale anti-contagion policies on the covid-19 pandemic. Nature 584 (7820), 262–267.

Ivanov, M., 2019. Exhaled air speed measurements of respiratory air flow, generated by ten different human subjects, under uncontrolled conditions. In: E3S Web of Conferences. Vol. 111. EDP Sciences.

Jaeger, M. J., Matthys, H., 1968. The pattern of flow in the upper human airways. Respiration physiology 6 (1), 113–127.

Jayaweera, M., Perera, H., Gunawardana, B., Manatunge, J., 2020. Transmission of covid-19 virus by droplets and aerosols: A critical review on the unresolved dichotomy. Environmental Research, 109819.

Johnson, G., Morawska, L., Ristovski, Z., Hargreaves, M., Mengersen, K., Chao, C. Y. H., Wan, M., Li, Y., Xie, X., Katoshevski, D., et al., 2011. Modality of human expired aerosol size distributions. Journal of Aerosol Science 42 (12), 839–851.

Johnson, G. R., Morawska, L., 2009. The mechanism of breath aerosol formation. Journal of Aerosol Medicine and Pulmonary Drug Delivery 22 (3), 229–237.

Kera, T., Maruyama, H., 2005. The effect of posture on respiratory activity of the abdominal muscles. Journal of physiological anthropology and applied human science 24 (4), 259–265.

Kinnunen, T., Koskela, M., 1991. Antibacterial and antifungal properties of propylene glycol, hexylene glycol, and 1, 3-butylene glycol in vitro. Acta dermato-venereologica 71 (2), 148.

Klompas, M., Baker, M. A., Rhee, C., 2020. Airborne transmission of sars-cov-2: theoretical considerations and available evidence. Jama.

Kulkarni P, B. P. A., K, W. (Eds.), 2011. Aerosol Measurement, Principles, Techniques, and Applications. John Wiley & Sons.

Lechasseur, A., Altmejd, S., Turgeon, N., Buonanno, G., Morawska, L., Brunet, D., Duchaine, C., Morissette, M. C., 2019. Variations in coil temperature/power and e-liquid constituents change size and lung deposition of particles emitted by an electronic cigarette. Physiological reports 7 (10), e14093.

Li, Y., Qian, H., Hang, J., Chen, X., Hong, L., Liang, P., Li, J., Xiao, S., Wei, J., Liu, L., et al., 2020. Evidence for probable aerosol transmission of sars-cov-2 in a poorly ventilated restaurant. medRxiv.

Liu, J., Liang, Q., Oldham, M. J., Rostami, A. A., Wagner, K. A., Gillman, I., Patel, P., Savioz, R., Sarkar, M., 2017. Determination of selected chemical levels in room air and on surfaces after the use of cartridge-and tank-based e-vapor products or conventional cigarettes. International journal of environmental research and public health 14 (9), 969.

Liu, Y., Ning, Z., Chen, Y., Guo, M., Liu, Y., Gali, N. K., Sun, L., Duan, Y., Cai, J., Westerdahl, D., et al., 2020. Aerodynamic analysis of sars-cov-2 in two wuhan hospitals. Nature 582 (7813), 557–560.

Lu, J., Gu, J., Li, K., Xu, C., Su, W., Lai, Z., Zhou, D., Yu, C., Xu, B., Yang, Z., 2020. Covid-19 outbreak associated with air conditioning in restaurant, guangzhou, china, 2020. Emerging infectious diseases 26 (7), 1628.

Manigrasso, M., Buonanno, G., Fuoco, F. C., Stabile, L., Avino, P., 2015. Aerosol deposition doses in the human respiratory tree of electronic cigarette smokers. Environmental Pollution 196, 257–267.

Marcolli, C., Peter, T., 2005. Water activity in polyol/water systems: new unifac parameterization.

Marian, C., O'Connor, R. J., Djordjevic, M. V., Rees, V. W., Hatsukami, D. K., Shields, P. G., 2009. Reconciling human smoking behavior and machine smoking patterns: implications for understanding smoking behavior and the impact on laboratory studies. Cancer Epidemiology and Prevention Biomarkers 18 (12), 3305–3320.

Martonen, T., 1992. Deposition patterns of cigarette smoke in human airways. American Industrial Hygiene Association Journal 53 (1), 6–18.

Martuzevicius, D., Prasauskas, T., Setyan, A., O'Connell, G., Cahours, X., Julien, R., Colard, S., 2019. Characterization of the spatial and temporal dispersion differences between exhaled e-cigarette mist and cigarette smoke. Nicotine and Tobacco Research 21 (10), 1371–1377.

Mather, J., McClure, A., 1945. Experiences with the use of propylene glycol as a bactericidal aerosol in an rcaf barracks. Canadian Journal of Public Health/Revue Canadienne de Sante'e Publique 36 (5), 181–187.

Matthews, T., Thompson, C., Wilson, D., Hawthorne, A., Mage, D., 1989. Air velocities inside domestic environments: an important parameter in the study of indoor air quality and climate. Environment International 15 (1-6), 545–550.

McAdam, K., Davis, P., Ashmore, L., Eaton, D., Jakaj, B., Eldridge, A., Liu, C., 2019. Influence of machine-based puffing parameters on aerosol and smoke emissions from next generation nicotine inhalation products. Regulatory Toxicology and Pharmacology 101, 156–165.

McNeill, A., Brose, L. S., Calder, R., Bauld, L., Robson, D., 2018. Evidence review of e-cigarettes and heated tobacco products 2018. A report commissioned by Public Health England. London: Public Health England 6.

Mikheev, V. B., Brinkman, M. C., Granville, C. A., Gordon, S. M., Clark, P. I., 2016. Real-time measurement of electronic cigarette aerosol size distribution and metals content analysis. Nicotine & Tobacco Research 18 (9), 1895–1902.

Morawska, L., Cao, J., 2020. Airborne transmission of sars-cov-2: The world should face the reality. Environment International, 105730.

Morawska, L., Johnson, G., Ristovski, Z., Hargreaves, M., Mengersen, K., Corbett, S., Chao, C. Y. H., Li, Y., Katoshevski, D., 2009. Size distribution and sites of origin of droplets expelled from the human respiratory tract during expiratory activities. Journal of Aerosol Science 40 (3), 256–269.

Morawska, L., Milton, D. K., 2020. It is time to address airborne transmission of coronavirus disease 2019 (covid-19). Clinical Infectious Diseases.

Morton, B., Nguyen, K., Cresswell, R., 1994. Similarity and self-similarity in the motion of thermals and puffs. In: Recent research advances in the fluid mechanics of turbulent jets and plumes. Springer, pp. 89–116.

Nalawade, T. M., Bhat, K., Sogi, S. H., 2015. Bactericidal activity of propylene glycol, glycerine, polyethylene glycol 400, and polyethylene glycol 1000 against selected microorganisms. Journal of international society of preventive & community dentistry 5 (2), 114.

Nazaroff, W. W., 2004. Indoor particle dynamics. Indoor air 14 (Supplement 7), 175–183.

Nicas, M., Nazaroff, W. W., Hubbard, A., 2005. Toward understanding the risk of secondary airborne infection: emission of respirable pathogens. Journal of occupational and environmental hygiene 2 (3), 143–154.

Nil, R., Woodson, P. P., Bättig, K., 1986. Smoking behaviour and personality patterns of smokers with low and high co absorption. Clinical science 71 (5), 595–603.

Organization, W. H., et al., 2020. Transmission of sars-cov-2: implications for infection prevention precautions: scientific brief, 09 july 2020. Tech. rep., World Health Organization.

Palmisani, J., Di Gilio, A., Palmieri, L., Abenavoli, C., Famele, M., Draisci, R., de Gennaro, G., 2019. Evaluation of second-hand exposure to electronic cigarette vaping under a real scenario: Measurements of ultrafine particle number concentration and size distribution and comparison with traditional tobacco smoke. Toxics 7 (4), 59.

Pankow, J. F., 2017. Calculating compound dependent gas-droplet distributions in aerosols of propylene glycol and glycerol from electronic cigarettes. Journal of aerosol science 107, 9–13.

Papineni, R. S., Rosenthal, F. S., 1997. The size distribution of droplets in the exhaled breath of healthy human subjects. Journal of Aerosol Medicine 10 (2), 105–116.

Polosa, R., O'Leary, R., Tashkin, D., Emma, R., Caruso, M., 2019. The effect of e-cigarette aerosol emissions on respiratory health: a narrative review. Expert review of respiratory medicine 13 (9), 899–915.

Pope, S. B., 2001. Turbulent flows.

Puck, T. T., 1947a. The mechanism of aerial disinfection by glycols and other chemical agents: I. demonstration that the germicidal action occurs through the agency of the vapor phase. The Journal of experimental medicine 85 (6), 729.

Puck, T. T., 1947b. The mechanism of aerial disinfection by glycols and other chemical agents: Ii. an analysis of the factors governing the efficiency of chemical disinfection of the air. The Journal of experimental medicine 85 (6), 741–757.

Puck, T. T., Robertson, O., Lemon, H. M., 1943. The bactericidal action of propylene glycol vapor on microorganisms suspended in air: ii. the influence of various factors on the activity of the vapor. The Journal of experimental medicine 78 (5), 387–406.

Rajaratnam, N., 1976. Turbulent jets. Elsevier.

RCP, 2016. Nicotine without smoke Tobacco harm reduction. Royal College of Physicians of London.

Robinson, J. H., Pritchard, W. S., Davis, R. A., 1992. Psychopharmacological effects of smoking a cigarette with typical "tar" and carbon monoxide yields but minimal nicotine. Psychopharmacology 108 (4), 466–472.

Rodenstein, D. O., Mercenier, C., Stănescu, D. C., 1985. Influence of the respiratory route on the resting breathing pattern in humans. American Review of Respiratory Disease 131 (1), 163–166.

Rodenstein, D. O., Stănescu, D. C., 1985. Pattern of inhalation of tobacco smoke in pipe, cigarette, and never smokers. American Review of Respiratory Disease 132 (3), 628–632.

Rowe, R. C., Sheskey, P., Quinn, M., 2009. Handbook of pharmaceutical excipients. Libros Digitales-Pharmaceutical Press.

Ruzer, L. S., Harley, N. H., 2012. Aerosols handbook: measurement, dosimetry, and health effects. CRC press.

Samburova, V., Bhattarai, C., Strickland, M., Darrow, L., Angermann, J., Son, Y., Khlystov, A., 2018. Aldehydes in exhaled breath during e-cigarette vaping: pilot study results. Toxics 6 (3), 46.

Sangras, R., Kwon, O., Faeth, G., 2002. Self-preserving properties of unsteady round nonbuoyant turbulent starting jets and puffs in still fluids. J. Heat Transfer 124 (3), 460–469.

Sangras, R., Kwon, O., Faeth, G., 2003. Erratum: Self-preserving properties of unsteady round nonbuoyant turbulent starting jets and puffs in still fluids. J. Heat Transfer 125 (3), 204–205.

Scharfman, B., Techet, A., Bush, J., Bourouiba, L., 2016. Visualization of sneeze ejecta: steps of fluid fragmentation leading to respiratory droplets. Experiments in Fluids 57 (2), 24.

Schwarz, K., Biller, H., Windt, H., Koch, W., Hohlfeld, J. M., 2010. Characterization of exhaled particles from the healthy human lung - a systematic analysis in relation to pulmonary function variables. Journal of aerosol medicine and pulmonary drug delivery 23 (6), 371–379.

Schwarz, K., Biller, H., Windt, H., Koch, W., Hohlfeld, J. M., 2015. Characterization of exhaled particles from the human lungs in airway obstruction. Journal of aerosol medicine and pulmonary drug delivery 28 (1), 52–58.

Scungio, M., Stabile, L., Buonanno, G., 2018. Measurements of electronic cigarette-generated particles for the evaluation of lung cancer risk of active and passive users. Journal of Aerosol Science 115, 1–11.

Shen, Y., Li, C., Martinez, L., Chen, Z., 2020. Airborne transmission of covid-19: epidemiologic evidence from two outbreak investigations.

Shin, D.-h., Aspden, A., Richardson, E. S., 2017. Self-similar properties of decelerating turbulent jets. Journal of Fluid Mechanics 833.

Shiu, E. Y., Leung, N. H., Cowling, B. J., 2019. Controversy around airborne versus droplet transmission of respiratory viruses: implication for infection prevention. Current opinion in infectious diseases 32 (4), 372–379.

Shoaib, A. M., Bhran, A. A., Hamed, M. F., 2016. Application of compact mixer technique for khalda gas dehydration plant. Int. J. Eng. Tech. Res 4, 40–47.

Sickbert-Bennett, E. E., Samet, J. M., Clapp, P. W., Chen, H., Berntsen, J., Zeman, K. L., Tong, H., Weber, D. J., Bennett, W. D., 2020. Filtration efficiency of hospital face mask alternatives available for use during the covid-19 pandemic. JAMA Internal Medicine 180 (12), 1607–1612.

Sosnowski, T. R., Kramek-Romanowska, K., 2016. Predicted deposition of e-cigarette aerosol in the human lungs. Journal of aerosol medicine and pulmonary drug delivery 29 (3), 299–309.

Sosnowski, T. R., Odziomek, M., 2018. Particle size dynamics: toward a better understanding of electronic cigarette aerosol interactions with the respiratory system. Frontiers in physiology 9, 853.

Soulet, S., Duquesne, M., Toutain, J., Pairaud, C., Mercury, M., 2019. Impact of vaping regimens on electronic cigarette efficiency. International Journal of Environmental Research and Public Health 16 (23), 4753.

Spindle, T. R., Hiler, M. M., Breland, A. B., Karaoghlanian, N. V., Shihadeh, A. L., Eissenberg, T., 2017. The influence of a mouthpiece-based topography measurement device on electronic cigarette user's plasma nicotine concentration, heart rate, and subjective effects under directed and ad libitum use conditions. Nicotine & Tobacco Research 19 (4), 469–476.

St. Helen, G., Havel, C., Dempsey, D. A., Jacob III, P., Benowitz, N. L., 2016. Nicotine delivery, retention and pharmacokinetics from various electronic cigarettes. Addiction 111 (3), 535–544.

Stadnytskyi, V., Bax, C. E., Bax, A., Anfinrud, P., 2020. The airborne lifetime of small speech droplets and their potential importance in sars-cov-2 transmission. Proceedings of the National Academy of Sciences 117 (22), 11875–11877.

Sussman, R. A., Golberstein, E., Polosa, R., 2020. Aerial transmission of the sars-cov-2 virus through environmental e-cigarette aerosol: is it plausible? "Qeios".

Sze To, G. N., Wan, M., Chao, C. Y. H., Wei, F., Yu, S., Kwan, J., 2008. A methodology for estimating airborne virus exposures in indoor environments using the spatial distribution of expiratory aerosols and virus viability characteristics. Indoor air 18 (5), 425–438.

Tcharkhtchi, A., Abbasnezhad, N., Seydani, M. Z., Zirak, N., Farzaneh, S., Shirinbayan, M., 2020. An overview of filtration efficiency through the masks: Mechanisms of the aerosols penetration. Bioactive materials 6 (1), 106–122.

Tobin, M. J., Jenouri, G., Sackner, M. A., 1982a. Subjective and objective measurement of cigarette smoke inhalation. Chest 82 (6), 696–700.

Tobin, M. J., Schneider, A. W., Sackner, M. A., 1982b. Breathing pattern during and after smoking cigarettes. Clinical Science 63 (5), 473–483.

Ueki, H., Furusawa, Y., Iwatsuki-Horimoto, K., Imai, M., Kabata, H., Nishimura, H., Kawaoka, Y., 2020. Effectiveness of face masks in preventing airborne transmission of sars-cov-2. MSphere 5 (5).

Van Doremalen, N., Bushmaker, T., Morris, D. H., Holbrook, M. G., Gamble, A., Williamson, B. N., Tamin, A., Harcourt, J. L., Thornburg, N. J., Gerber, S. I., et al., 2020. Aerosol and surface stability of sars-cov-2 as compared with sars-cov-1. New England Journal of Medicine 382 (16), 1564–1567.

Vas, C. A., Yurteri, C. Ü., Dickens, C. J., Prasad, K., 2015. Development and characterisation of a smoking behaviour measurement system. Beiträge zur Tabakforschung International/Contributions to Tobacco Research 26 (5), 219–231.

Vuorinen, V., Aarnio, M., Alava, M., Alopaeus, V., Atanasova, N., Auvinen, M., Balasubramanian, N., Bordbar, H., Erästö, P., Grande, R., et al., 2020. Modelling aerosol transport and virus exposure with numerical simulations in relation to sars-cov-2 transmission by inhalation indoors. Safety Science 130, 104866.

Wang, J., Chow, T.-T., 2011. Numerical investigation of influence of human walking on dispersion and deposition of expiratory droplets in airborne infection isolation room. Building and Environment 46 (10), 1993–2002.

Weber, T. P., Stilianakis, N. I., 2008. Inactivation of influenza a viruses in the environment and modes of transmission: a critical review. Journal of infection 57 (5), 361–373.

Wei, J., Li, Y., 2015. Enhanced spread of expiratory droplets by turbulence in a cough jet. Building and Environment 93, 86–96.

Wei, J., Li, Y., 2016. Airborne spread of infectious agents in the indoor environment. American journal of infection control 44 (9), S102–S108.

Weissman, C., Askanazi, J., Milic-Emili, J., Kinney, J. M., 1984. Effect of respiratory apparatus on respiration. Journal of Applied Physiology 57 (2), 475–480.

Wheatley, J., Amis, T., Engel, L., 1991. Nasal and oral airway pressure-flow relationships. Journal of Applied Physiology 71 (6), 2317–2324.

Woodman, G., Newman, S., Pavia, D., Clarke, S., 1986. Inhaled smoke volume, puffing indices and carbon monoxide uptake in asymptomatic cigarette smokers. Clinical Science 71 (4), 421–427.

Wurie, F., de Waroux, O. L. P., Brande, M., DeHaan, W., 2013. Characteristics of exhaled particle production in healthy volunteers: possible implications for infectious disease.

Xu, C., 2018. Characterizing human breathing and its interactions with room ventilation. Ph.D. thesis, phD supervisor: Associate Prof. Li Liu, Aalborg University Assistant PhD supervisors: Prof. Peter V. Nielsen, Aalborg University Prof. Guangcai Gong, Hunan University.

Xu, C., Nielsen, P., Gong, G., Liu, L., Jensen, R., 2015. Measuring the exhaled breath of a manikin and human subjects. Indoor Air 25 (2), 188–197.

Xu, C., Nielsen, P. V., Liu, L., Jensen, R. L., Gong, G., 2017. Human exhalation characterization with the aid of schlieren imaging technique. Building and Environment 112, 190–199.

Yeoh, G. H., Tu, J., 2019. Computational techniques for multiphase flows. Butterworth-Heinemann.

Yu, I. T., Li, Y., Wong, T. W., Tam, W., Chan, A. T., Lee, J. H., Leung, D. Y., Ho, T., 2004. Evidence of airborne transmission of the severe acute respiratory syndrome virus. New England Journal of Medicine 350 (17), 1731–1739.

Zhang, H., Li, D., Xie, L., Xiao, Y., 2015. Documentary research of human respiratory droplet characteristics. Procedia Engineering 121, 1365–1374.

Zhao, T., Nguyen, C., Lin, C.-H., Middlekauff, H. R., Peters, K., Moheimani, R., Guo, Q., Zhu, Y., 2017. Characteristics of secondhand electronic cigarette aerosols from active human use. Aerosol Science and Technology 51 (12), 1368–1376.

Zhao, T., Shu, S., Guo, Q., Zhu, Y., 2016. Effects of design parameters and puff topography on heating coil temperature and mainstream aerosols in electronic cigarettes. Atmospheric Environment 134, 61–69.

Zhou, J., Otter, J. A., Price, J. R., Cimpeanu, C., Garcia, D. M., 2020. Investigating sars-cov-2 surface and air contamination in an acute healthcare setting during. Emerging infectious diseases, 26.

Zhu, S., Yang, J.-H., Kato, S., 2006. Investigation into airborne transport characteristics of airflow due to coughing in a stagnant indoor environment. ASHRAE transactions 112 (1).